

Forensics-Bench: A Comprehensive Forgery Detection Benchmark Suite for Large Vision Language Models

Jin Wang^{1,*}, Chenghui Lv^{5,4,*}, Xian Li^{6,4}, Shichao Dong⁷, Huadong Li⁸, Kelu Yao⁴, Chao Li⁴, Wenqi Shao³, Ping Luo^{1,2,†}

¹The University of Hong Kong ²HKU Shanghai Intelligent Computing Research Center

³Shanghai AI Laboratory ⁴Zhejiang Laboratory ⁵Hangzhou Institute for Advanced Study

⁶Zhejiang University ⁷Alibaba, Beijing, China ⁸MEGVII Technology

Abstract

Recently, the rapid development of AIGC has significantly boosted the diversities of fake media spread in the Internet, posing unprecedented threats to social security, politics, law, and etc. To detect the ever-increasingly **diverse** malicious fake media in the new era of AIGC, recent studies have proposed to exploit Large Vision Language Models (LVLMs) to design **robust** forgery detectors due to their impressive performance on a **wide** range of multimodal tasks. However, it still lacks a comprehensive benchmark designed to comprehensively assess LVLMs' discerning capabilities on forgery media. To fill this gap, we present *Forensics-Bench*, a new forgery detection evaluation benchmark suite to assess LVLMs across massive forgery detection tasks, requiring comprehensive recognition, location and reasoning capabilities on diverse forgeries. *Forensics-Bench* comprises 63,292 meticulously curated multi-choice visual questions, covering 112 unique forgery detection types from 5 perspectives: forgery semantics, forgery modalities, forgery tasks, forgery types and forgery models. We conduct thorough evaluations on 22 open-sourced LVLMs and 3 proprietary models GPT-4o, Gemini 1.5 Pro, and Claude 3.5 Sonnet, highlighting the significant challenges of comprehensive forgery detection posed by *Forensics-Bench*. We anticipate that *Forensics-Bench* will motivate the community to advance the frontier of LVLMs, striving for all-around forgery detectors in the era of AIGC. The deliverables will be updated [here](#).

1. Introduction

In recent years, with the rapid development of AI-generated content (AIGC) technology [23, 28, 33], the barrier to creating fake media has been significantly lowered for the

general public. As a result, a large amount of various synthetic media has flooded the Internet, which poses unprecedented threats to politics, law, and social security, such as the malicious dissemination of deepfakes [24, 40] and misinformation [60]. To address such situations, researchers have proposed numerous forgery detection methods [20, 30, 45, 78, 81, 112], aiming to filter out synthetic media as much as possible. Nevertheless, the synthetic media nowadays can be incredibly **diverse**, which may encompass different modalities, depict various semantics, and be created/manipulated with different AI models, etc. Thus, designing a **generalized** forgery detector with such comprehensive discerning capabilities becomes a crucial and urgent task in this new era of AIGC, posing significant challenges to the research community.

In the meantime, Large Vision Language Models (LVLMs) [2, 8, 53, 69, 84, 107, 108] have achieved remarkable progress in a **wide** range of multimodal tasks, such as visual recognition and visual captioning, which reignites the discussion of artificial general intelligence (AGI) [65]. These promising generalization capabilities make LVLMs a compelling solution for distinguishing increasingly diverse synthetic media [6, 35, 37, 55, 72, 110]. However, it still lacks a comprehensive evaluation benchmark to assess LVLMs' ability to recognize synthetic media, which hinders the applications of LVLMs on forgery detection and thus further impedes the continuous progress of LVLMs towards the next level of AGI [65]. To this end, a line of work [47, 56, 80, 88, 113] attempted to bridge this gap with different evaluation benchmarks, but they only cover a limited range of synthetic media, such as out-of-context forgeries [60] and diffusion-based forgeries [74], which restricts their comprehensiveness in revealing the full extent of LVLMs' forgery detection capabilities.

To drive the research in this direction, we introduce *Forensics-Bench*, a new forgery detection benchmark suite for comprehensively evaluating the capabilities of LVLMs

*Equal contribution (primary contact: wj0529@connect.hku.hk)

†Corresponding author

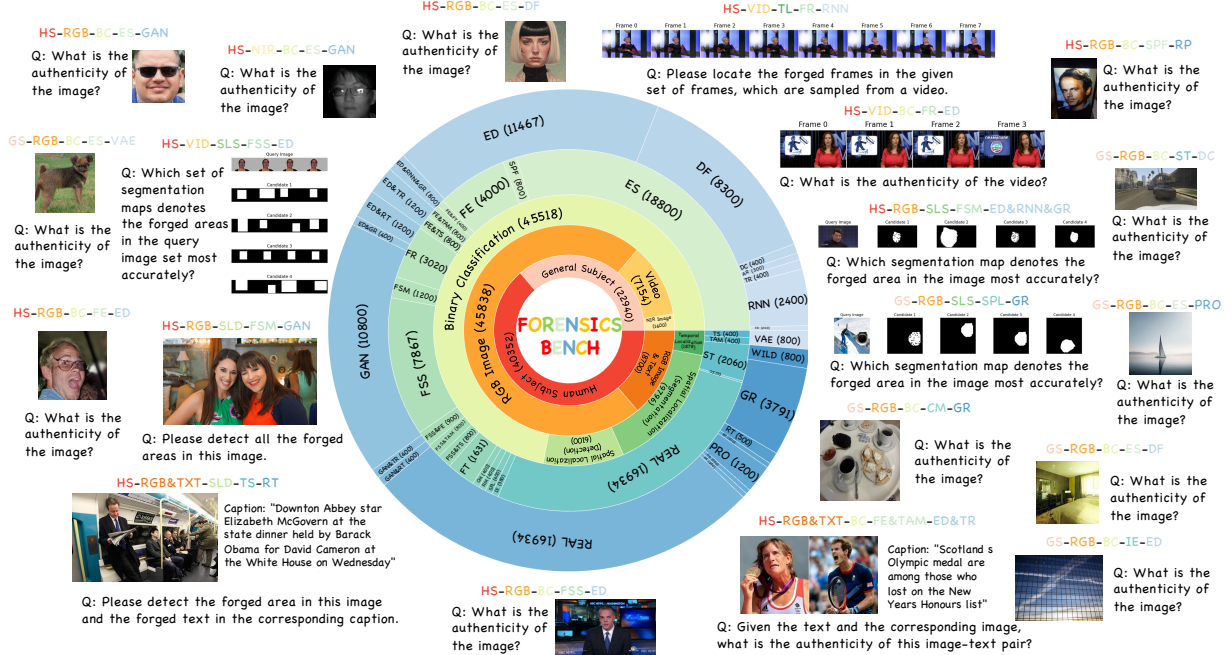


Figure 1. Overview of Forensics-Bench. Forensics-Bench consists of 63K samples, covering 112 unique forgery detection types from five different perspectives characterizing forgeries. As shown in different rings from inside out, these five perspectives include **forgery semantics**, **forgery modalities**, **forgery tasks**, **forgery types** and **forgery models**. From the view of **forgery semantics**, Forensics-Bench includes data featuring: $HS \rightarrow Human\ Subject$ and $GS \rightarrow General\ subject$. From the view of **forgery modalities**, Forensics-Bench includes data featuring: $RGB\&TXT \rightarrow RGB\ Image\ \&\ Text$, $VID \rightarrow Video$ and etc. From the view of **forgery tasks**, Forensics-Bench includes data featuring: $TL \rightarrow Temporal\ Localization$, $SLS \rightarrow Spatial\ Localization\ (Segmentation)$, $BC \rightarrow Binary\ Classification$ and etc. From the view of **forgery types**, Forensics-Bench includes data featuring: $TS \rightarrow Text\ Swap$, $FSS \rightarrow Face\ Swap\ (Single\ Face)$, $ES \rightarrow Entire\ Synthesis$ and etc. From the view of **forgery models**, Forensics-Bench includes data generated from: $GAN \rightarrow Generative\ Adversarial\ Models$, $DF \rightarrow Diffusion\ models$, $VAE \rightarrow Variational\ Auto-Encoders$ and etc. Forensics-Bench enables comprehensive evaluations of LVLMs on versatile forgery detection types in the evolving era of AIGC. Please see Appendix 6 for more detailed abbreviations.

in the context of forgery detection. To this end, Forensics-Bench is meticulously curated to cover forgeries as various as possible, consisting of 63K multi-choice visual questions and covering 112 unique forgery detection types in statistics. Specifically, the **breadth** of Forensics-Bench addresses five perspectives: 1) *Different forgery modalities*, including RGB images, NIR images, videos and texts. 2) *Various semantics*, covering both human subjects and other general subjects. 3) *Created/manipulated with different AI models*, such as GANs, diffusion models, VAE and etc. 4) *Various task types*, including forgery binary classification, forgery spatial localization and forgery temporal localization. 5) *Versatile forgery types*, such as face swap, face attribute editing, face reenactment and etc. Such diversity in Forensics-Bench demands LVLMs to equip with comprehensive capabilities on discerning various forgeries, underscoring the significant challenges posed by AIGC technology nowadays. Please see Figure 1 for details.

In experiments, we evaluated 22 publicly available LVLMs and 3 proprietary models based on Forensics-Bench to comprehensively compare their capabilities in forgery de-

tection. We summarized our findings as follows.

- We find that Forensics-Bench presented significant challenges to state-of-the-art LVLMs, the best of which only achieved 66.7% overall accuracy, highlighting the unique difficulty of robust forgery detection.
- Among various forgery types, LVLMs demonstrated a significant bias in their performance: they excelled at certain forgery types like spoofing and style translation (close to 100%), but performed poorly on others like face swap (multiple faces) and face editing (lower than 55%). This outcome uncovered the partial understanding LVLMs have regarding different forgery types.
- In different forgery detection tasks, LVLMs generally demonstrated better performance on classification tasks, while struggling with spatial and temporal localization tasks.
- Forgeries synthesized by popular AI models, we find that current LVLMs performed better on forgeries output by diffusion models compared with those generated by GANs. Such results exposed the limitations in LVLMs' capabilities in discerning forgeries provided by different

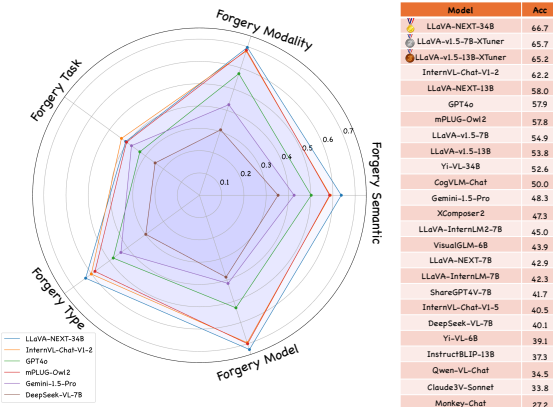


Figure 2. Forensics-Bench evaluation results of Large Vision Language Models (LVLMs). We visualize evaluation results of representative LVLMs in five Forensics-Bench perspectives on the left side and present the overall leaderboard results on the right side. For detailed quantitative results, please refer to Table 2.

AI models.

Overall, the contributions of this paper are summarized as follows. i) We introduce a novel benchmark, Forensics-Bench, compiling 112 diverse forgery detection types based on five perspectives characterizing different forgeries. ii) We conduct a thorough and comprehensive evaluation of 25 state-of-the-art LVLMs on Forensics-Bench. Through extensive experiments, we discover significant variability in LVLMs’ performance across different forgery detection types, exposing the limitations of their capabilities. iii) We provide multi-faceted analytical experiments related to forgery detection, such as forgery detection under perturbations and forgery attribution, further showcasing the limitations of LVLMs’ understanding of forgeries. We hope that Forensics-Bench can aid researchers in gaining a deeper understanding of the LVLMs’ capabilities on forgery detection, offering insights for future designs and solutions.

2. Related Work

2.1. Forgery Detection

With the rapid advancement of AIGC technology [23, 28, 33], synthetic media has become increasingly realistic and indistinguishable to the public. Malicious users can easily exploit these techniques to spread fake news, forge judicial evidence, and tarnish the reputations of celebrities, posing significant challenges to social security. In response, many researchers have proposed a variety of methods to detect synthetic media, aiming to ensure the authenticity and reliability of collected content [16, 19, 63, 83]. However, previous approaches often lacked generalization capabilities, struggling to maintain performance when faced with unseen forgeries [3, 18, 46, 75, 95]. To this end, numerous methods

Benchmark	Forgery Data Collection				
	# Sample	Semantic	# Modality	# Task	# Model
FakeBench [47]	54K	Huann & General	2	4	1
MMFakeBench [56]	11K	Human	2	1	12
MFC-Bench [88]	35K	Human & General	2	1	9
Forensics-Bench	63K	Human & General	4	4	22

Table 1. The comparison between Forensics-Bench and existing evaluation benchmarks for Large Vision Language Models in the context of forgery detection.

[20, 25, 30, 44, 45, 78, 81, 82, 96, 97, 111, 112] have been proposed, expecting to increase the generalization capabilities of current forgery detectors. However, this challenge was significantly amplified by the recent evolution of diverse AIGC techniques [23, 28, 33, 100], which drastically increased the diversity and complexity of forgeries. Therefore, to support the development of robust forgery detectors, designing a comprehensive evaluation benchmark for all-round forgery detection has become an urgent necessity.

2.2. LVLMs and Benchmark

With the rapid advancement of Large Language Models (LLMs) [11, 68, 70, 86, 87, 98], there was a growing interest among researchers in enhancing the visual understanding capabilities of these models. The key to developing LVLMs lies in aligning visual content with language based on the foundation of LLMs. CLIP [73] was one of the pioneering works in this area, exploring contrastive learning with a large corpus of image-text pairs to align visual and language representations in a unified latent space. Subsequently, to improve the reception and comprehension of visual content by LLMs, Mini-GPT4 [115] directly connected the visual encoder with a frozen LLM using a multilayer perceptron (MLP). More recently, there has been a shift towards fine-tuning existing models through instruction tuning techniques [7, 14, 21, 52, 53, 61, 101]. For instance, LLaVA [53] fine-tuned models by constructing a 158K instruction-following dataset, ultimately endowing the model with excellent visual understanding capabilities.

To accurately assess the real capabilities of these LVLMs, a comprehensive and challenging benchmark [26, 43, 57, 77, 79, 94, 104, 105] is essential. Early single-task benchmarks [29, 62, 79], such as MS-COCO [79] and VQA [29], typically evaluated LVLMs on specific aspects. As LVLMs became capable of handling an increasing variety of tasks, more comprehensive benchmarks [10, 26, 43, 57, 77, 94, 104, 105], like MM-Bench [57], MMMU [105], and MMT-Bench [102], have been proposed to evaluate models across multiple dimensions. These benchmarks, with their broad range of tasks, comprehensively tested the true abilities of LVLMs, advancing our understanding of their capability boundaries and providing critical insights for further improvements. However, in the context of forgery detection, there still lacks a comprehen-

sive evaluation benchmark to holistically assess the forgery detection capabilities of LVLMs in fine-grained perspectives.

2.3. Forgery Detection and LVLMs

In recent years, leveraging Large Vision-Language Models (LVLMs) for forgery detection has gained significant attention due to their exceptional capabilities in understanding versatile visual content. A series of studies [6, 35, 37, 50, 55, 72, 80, 93] have demonstrated the effectiveness of LVLMs in forgery detection tasks. To better evaluate the capabilities of LVLMs in this domain, several benchmarks [47, 56, 80, 88, 113] have been introduced to assess their effectiveness. However, these evaluation benchmarks were usually limited in scope, assessing only partial capabilities of LVLMs in the field of forgery detection. To address this limitation, we propose Forensics-Bench, which compiles 63K multimodal questions across 112 diverse forgery detection types, providing a comprehensive evaluation testbed for current state-of-the-art LVLMs.

3. Forensics-Bench

In this section, we present the main components of Forensics-Bench. In Section 3.1, we first introduce the design principles of Forensics-Bench. Next, in Section 3.2, we elaborate the detailed construction process of Forensics-Bench and give a brief overview of Forensics-Bench.

3.1. Benchmark Design

To provide a comprehensive testbed for Large Vision Language Models (LVLMs) in the context of forgery detection, we propose to design our Forensics-Bench from five perspectives to characterize different forgeries, consisting of forgery semantics, forgery modalities, forgery tasks, forgery types, and forgery models.

Forgery semantics. Human subjects have been a long-standing focus of previous forgery detection studies [18, 36, 46, 75], considering the significant threats of deepfakes posed to social security. Besides, considering the unprecedented capabilities of recent generative models, such as Stable Diffusion Models [71, 74], newly-generated media can contain versatile semantics given the free space of textual prompts. Thus, it is of great importance that future forgery detectors should show no bias towards certain types of content illustrated in forged images/videos. Therefore, we propose to classify data into human subjects and other general subjects in Forensics-Bench, to evaluate LVLMs' performance when encountering different semantics.

Forgery modalities. In recent years, the modalities of forgeries have become increasingly various [5, 38, 46, 75, 78, 91, 106], which may cause greater impact on our daily life. To this end, we propose to characterize the forgery data based on different modalities, including RGB images, NIR

images, videos, and texts, to assess whether LVLMs show significant performance variations across these modalities, thereby revealing their preferences.

Forgery tasks. The general goal of forgery detection is to recognize whether the given media is real or fake, namely, conducting binary classifications [67, 75, 89, 92]. Besides, previous studies [32, 42] have focused on localizing the forged areas on images/videos, providing more finer and explainable information for users. To this end, from this perspective, we propose to cover 4 common forgery detection tasks, namely forgery binary classification, forgery spatial localization (segmentation masks), forgery spatial localization (bounding boxes) and forgery temporal localization. This design encompasses most forgery detection scenarios, allowing for a detailed comparison of different LVLMs' performance across various tasks.

Forgery types. With a plethora of AIGC techniques coming in handy, malicious users nowadays can apply diverse operations into different forgeries. In this paper, we refer these kinds of operations as different forgery types. For instance, users can conduct face swap or face reenactment to any given human subject videos [75], or even directly synthesizing the whole video from scratch [41, 100]. To this end, we propose to classify the forgery data from the perspective of forgery types in Forensics-Bench. This includes entire synthesis, face spoofing, face editing, text attribute manipulation, text swap, face reenactment, face swap (multiple faces), face swap (single face), copy-move, removal, splicing, image enhancement, out-of-context, style translation, and different combinations of the above operations. Please see Appendix 8 for detailed descriptions of these forgery types. This comprehensive design can help to evaluate whether LVLMs maintain robust performance when faced with diverse and complex forgery types.

Forgery models. Another important research direction in forgery detection is to identify the forgery model that is applied to the given input [27, 32, 99]. This may presents continuous challenges to future forgery detectors as the generative models are constantly proposed and may be applied to generate forgeries. To this end, in our benchmark, we propose to collect samples generated from popular AI models, which includes Diffusion models, Encoder-Decoder, graphics-based models, GANs, VAEs, RNNs and etc. Please see Appendix 8 for detailed descriptions. This design can help to carefully analyze LVLMs' performance across data from various AI model sources.

3.2. Data Collection

Based on the above comprehensive benchmark design, we then collect our Forensics-Bench in a top-down hierarchy. As shown in Fig. 3, all co-authors first brainstorm and list common forgery semantics, forgery modalities, forgery tasks, forgery types and forgery models shown in previous

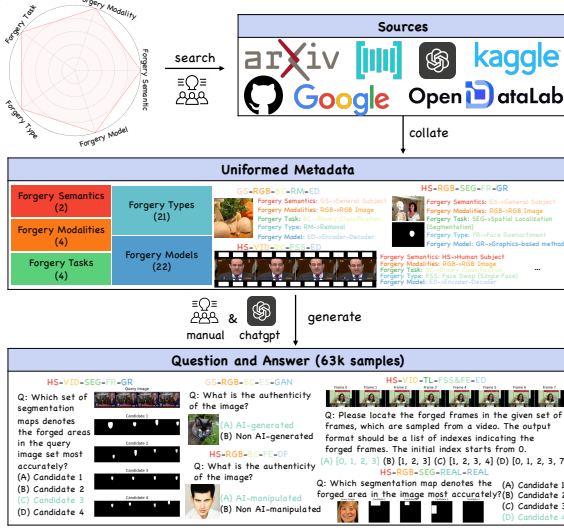


Figure 3. An illustration of the pipeline for data collection of Forensics-Bench. First, from the designed 5 perspectives of Forensics-Bench, we searched the related public available dataset from the Internet. Then, we collated the retrieved dataset into a uniformed metadata format. Finally, we either manually transformed original data into handcrafted Questions&Answers (Q&A) or proceed the Q&A transformation with the aid of ChatGPT. Forensics-Bench supports evaluations over a diverse kinds of forgeries across various perspectives. Please zoom in for better visualizations.

literature. Then, we retrieve the relevant public datasets for each listed item, covering forgery detections types as many as possible. Finally, we construct corresponding multi-choice Questions&Answers (Q&A) samples manually or with the aid of ChatGPT.

Dataset search. Considering the widespread of our benchmark design, we have gathered a comprehensive collection of datasets in the field of forgery detection, sourced from public available datasets and academic repositories. These sources are strategically selected to encompass a wide array of forgery data, ensuring the breadth of our dataset. Furthermore, we incorporate both synthetic and real-world data to approximately reflect the practical and complex challenges faced in contemporary forgery detections. These data sources are carefully listed in Appendix 7. After collection, we conduct a comprehensive cleansing and filtering process to enhance the quality and utility of the dataset. Note that we only exploit the test/validation set of the public datasets for data cleansing, ensuring that the collected data in Forensics-Bench is not seen by LVLMs as much as possible. Duplicates and low-quality samples are manually identified and removed to uphold high data quality standards. The forgery data across all sources is then standardized, followed by meticulous annotations and transformations to en-

sure correctness throughout the entire dataset construction.

Metadata structure. We standardized all the cleansed data to generate metadata, depicting the necessary meta-information of each forgery detection type. Typically, we randomly select 200 samples for each forgery detection type per public dataset for testing, recording key information within the metadata structure such as forgery types, forgery tasks, forgery models and etc. Considering the popularity of different forgery models, some forgery detection types may source from multiple public datasets, such as forgeries synthesized by diffusion models and GANs. Additionally, other details like image resolution and text-image pairings are also documented. For samples in the format of video modality, we uniformly extract frames from each forged video to record in the metadata. Ultimately, this metadata is exploited to generate multi-choice Questions&Answers (Q&A), thus assessing the capabilities of LVLMs in the context of forgery detection.

Question and Answer Generation. Based on the recorded metadata, we then generate corresponding multi-choice Questions&Answers based on manual rules or ChatGPT. Some examples are illustrated in Fig. 3. For example, for forgery binary classification task, some choices may include AI-generated/non AI-generated, or AI-manipulated/non AI-manipulated, depending on whether the media is entirely synthesized by AI models or modified by AI models based on real media. For forgery spatial localization tasks (segmentation masks), the wrong choices are generated by adding random perturbations to the ground truth. These choice designs can help reduce the ambiguity of the generated Questions&Answers and increase the relevance between correct answers and wrong answers, ensuring the fairness on the evaluation results of Forensics-Bench.

Dataset Statistics. Finally, Forensics-Bench consists of 63292 data samples, covering 46358 forgery samples and 16934 real samples, following the designed ratios of previous datasets [18, 46, 75] where the forgery samples accounts for the majority given the diversities of AIGC techniques. In Forensics-Bench, we cover 2 forgery semantics, 4 forgery modalities, 4 forgery tasks, 21 forgery types and 22 forgery models, comprehensively evaluating the perception, location and reasoning capabilities of LVLMs in the context of forgery detection. A detailed comparison with previous evaluation benchmarks for Large Vision Language Models in the context of forgery detection is provided in Table 1. To the best of our knowledge, Forensics-Bench is the largest forgery detection benchmark for LVLMs to date, featuring the most diverse forgeries and evaluation perspectives.

3.3. Other Evaluation Protocols

Thanks to the comprehensiveness of Forensics-Bench, we can further complement the evaluations of LVLMs’ forgery

detection capabilities with our benchmark. To this end, we further propose 2 extra evaluation protocols supported by Forensics-Bench, providing finer analyses on LVLMs’ abilities.

Protocol 1. Robust Forgery Detection. Inspired by previous studies [31, 36], we introduce common perturbations into the samples to evaluate the stability of LVLMs’ forgery detection capabilities in noisy real-life environments. These introduced perturbations are commonly seen on the Internet, consisting of change of color saturation, local block-wise distortion, change of color contrast, Gaussian blur, white Gaussian noise and JPEG compression, each of which features 5 different intensity levels. This evaluation protocol can help assess LVLMs’ forgery detection capabilities in real-life scenarios, exploring the potential of LVLMs for practical deployment.

Protocol 2. Forgery Attribution. Inspired by previous studies [27, 99], we can evaluate the forgery attribution capabilities of LVLMs owing to the forgery data in Forensics-Bench, which is generated/manipulated by a wide range of AI models. Specifically, we repurpose our questions in Forensics-Bench to ask LVLMs to identify the AI models that are applied to the given media. The wrong choices are randomly sampled from the 22 forgery models listed in Forensics-Bench. Note that we only repurpose the samples featuring forgery binary classifications in Forensics-Bench for this protocol. This evaluation perspective can help further analyze LVLMs’ forgery detection capabilities, providing explainable and detailed support for LVLMs’ answers.

4. Experiments

4.1. Experiment Setup

LVLM Models. With our proposed Forensics-Bench, we then conduct experiments to evaluate 22 open-sourced LVLMs, including LLaVA-NEXT-34B [54], LLaVA-v1.5-7B-XTuner [13], LLaVA-v1.5-13B-XTuner [13], InternVL-Chat-V1-2 [8, 86], LLaVA-NEXT-13B [54], mPLUG-Owl2 [101], LLaVA-v1.5-7B [52, 53], LLaVA-v1.5-13B [52, 53], Yi-VL-34B [103], CogVLM-Chat [90], XComposer2 [21], LLaVA-InternLM2-7B [13], VisualGLM-6B, LLaVA-NEXT-7B [54], LLaVA-InternLM-7B [13], ShareGPT4V-7B [7], InternVL-Chat-V1-5 [8, 86], DeepSeek-VL-7B [58], Yi-VL-6B [103], InstructBLIP-13B [14], Qwen-VL-Chat [2] and Monkey-Chat [48]. Besides, we also conduct evaluations on 3 proprietary models: GPT4o [69], Gemini 1.5 Pro [85] and Claude 3.5 Sonnet [1].

Evaluation Details. With the evaluation tool [22] provided in OpenCompass [12], we followed previous studies [64, 102] to conduct evaluations: 1) we first manually check whether the option letter appears in the LVLMs’ answers; 2) we then manually check whether the option content appears

Model	Overall	Semantic	Modality	Task	Type	Model
Proprietary Large Vision Language Models						
GPT4o	57.9	50.2	57.3	33.1	47.9	53.1
Gemini-1.5-Pro	48.3	42.6	42.7	37.8	43.7	41.6
Claude3V-Sonnet	33.8	28.4	28.5	32.1	29.9	28.9
Open-sourced Large Vision Language Models						
LLaVA-NEXT-34B	66.7	63.8	69.7	41.0	63.3	72.7
LLaVA-v1.5-7B-XTuner	65.7	61.2	68.3	41.9	58.2	66.8
LLaVA-v1.5-13B-XTuner	65.2	62.9	68.7	37.9	61.3	71.8
InternVL-Chat-V1-2	62.2	58.8	67.9	43.4	60.1	69.5
LLaVA-NEXT-13B	58.0	64.0	66.7	32.0	62.3	71.2
mPLUG-Owl2	57.8	58.5	68.4	40.5	58.1	70.0
LLaVA-v1.5-7B	54.9	61.6	68.7	37.1	64.0	70.8
LLaVA-v1.5-13B	53.8	52.7	64.2	34.1	55.6	63.7
Yi-VL-34B	52.6	47.2	53.6	39.7	41.2	51.6
CogVLM-Chat	50.0	44.1	49.5	32.2	45.4	52.0
XComposer2	47.3	42.2	43.8	28.3	42.9	48.4
LLaVA-InternLM2-7B	45.0	40.8	52.2	30.5	42.6	50.3
VisualGLM-6B	43.9	38.9	39.1	30.3	35.1	39.2
LLaVA-NEXT-7B	42.9	49.0	53.1	32.1	55.7	63.7
LLaVA-InternLM-7B	42.3	37.7	39.4	30.2	39.9	47.5
ShareGPT4V-7B	41.7	44.6	46.9	32.3	51.8	58.5
InternVL-Chat-V1-5	40.5	39.9	33.6	28.7	41.7	47.6
DeepSeek-VL-7B	40.1	35.4	30.8	24.6	29.8	38.6
Yi-VL-6B	39.1	38.2	39.4	30.7	39.4	48.1
InstructBLIP-13B	37.3	33.1	42.2	27.1	28.4	33.7
Qwen-VL-Chat	34.5	29.6	32.1	27.1	32.4	34.3
Monkey-Chat	27.2	18.6	18.1	20.6	19.2	21.2

Table 2. Quantitative results for 22 open-sourced LVLMs and 3 proprietary LVLMs across 5 perspectives of forgery detection are summarized. Accuracy is the metric. The overall score is calculated across all data in Forensics-Bench.

in the LVLMs’ answers; 3) we finally resort ChatGPT to help extract the matching option. If the above extractions still fail, we set the model’s answer as Z [105]. As for evaluation metrics, we use accuracy in our experiments.

4.2. Main Results

The main evaluation results are summarized in Table 2. The score in each perspective of Forensics-Bench design is the averaged accuracy over related samples. To this end, we have the following findings: 1) We find that Forensics-Bench presented significant challenges to state-of-the-art LVLMs. The best one (LLaVA-NEXT-34B) only achieved 66.7% overall accuracy on Forensics-Bench, underscoring the unique difficulty of generalized forgery detection. 2) We find that proprietary LVLMs (such as GPT-4o) demonstrated relatively weaker performance than open-sourced models, especially the series of LLaVA models, in the context of forgery detection. This is mostly because that proprietary LVLMs tend to response with more conservative answers, admitting that they can not conclude the authenticity

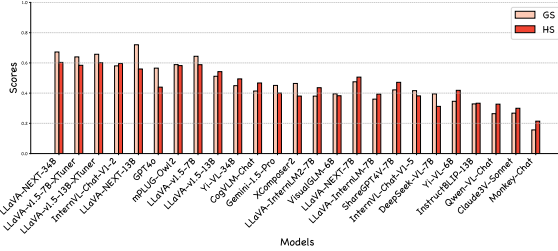


Figure 4. Results of Forensics-Bench from the perspective of *forgery semantics*. Most LVLMs did not demonstrate strong bias towards certain media content in terms of human subject *vs* general subject.

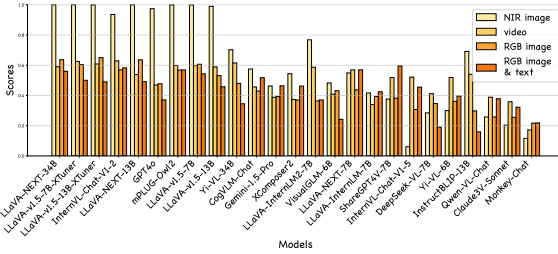


Figure 5. Results of Forensics-Bench from the perspective of *forgery modality*. Current LVLMs failed to perform well across all forgery modalities collected in Forensics-Bench.

of the input with strong confidence. 3) We further conduct detailed analyses from each perspective in our Forensics-Bench:

Analysis on forgery semantics. We illustrated the detailed performance of 25 LVLMs in Figure 4 from the perspective of forgery semantics. It can be seen that most LVLMs did not demonstrate significant bias towards certain content in terms of human subjects *vs* general subjects. This provide great starting points for the development of future all-round forgery detectors under the paradigm of LVLMs.

Analysis on forgery modalities. We showed the detailed performance of 25 LVLMs in Figure 5 from the perspective of forgery modalities. We find that top-performing LVLMs (such as LLaVA-NEXT-34B) achieved impressive binary classification performance on forgeries in the near-infrared (NIR) modality. Meanwhile, when the input content contains both RGB images and texts [78], these LVLMs struggled to performed well. It is still worth exploring to design robust forgery detectors excelled at different modalities.

Analysis on forgery tasks. The detailed performance of 25 LVLMs from the perspective of forgery tasks is shown in Figure 6. We find that most LVLMs demonstrated relatively great performance in the forgery binary classification (BC) task, while having difficulty maintaining strong performance in the tasks of forgery spatial localization (segmentation masks/bounding boxes) (SLS/SLD) and forgery

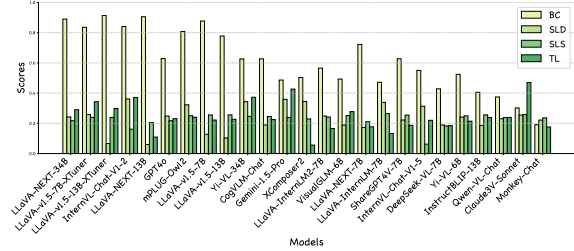


Figure 6. Results of Forensics-Bench from the perspective of *forgery task*. Current LVLMs performed well in forgery binary classification task, but struggled to maintain the performance over other forgery tasks designed in Forensics-Bench.

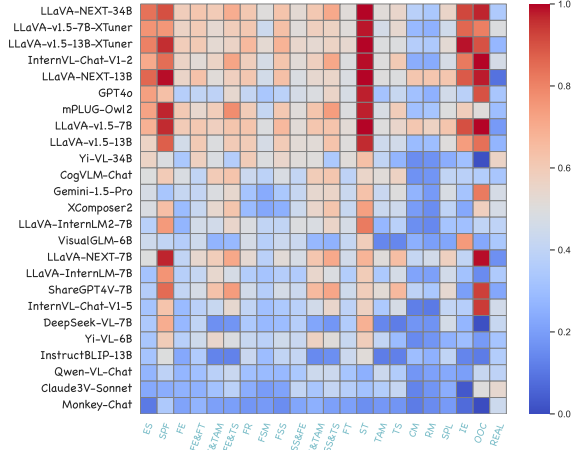


Figure 7. Results of Forensics-Bench from the perspective of *forgery type*. Current LVLMs still exhibited limitations in forgery detections across a wide range of forgery types.

temporal localization (TL). Such results reveal that most LVLMs still required improvements over location and reasoning capabilities in different forgery detection tasks.

Analysis on forgery types. The detailed performance of 25 LVLMs from the perspective of forgery types is illustrated in Figure 7. Firstly, we find that current LVLMs still found it challenging to perform well over a wide range of forgery types, such as face swap (multiple faces), copy-move (CM), removal (RM) and splicing (SPL). Second, we find that leading LVLMs like LLaVA series models already excelled in certain forgery types, such as face spoofing (SPF), image enhancement (IE), style translation (ST) and out-of-context (OOC), indicating their potential to grow into more generalized forgery detectors.

Analysis on forgery models. The detailed performance of 25 LVLMs from the perspective of forgery models is illustrated in Figure 8. It is noticeable that leading LVLMs achieved excellent performance at forgeries created with spoofing methods, such as 3D masks (3D) and paper cut (PC). Besides, for forgeries synthesized by popular AI mod-

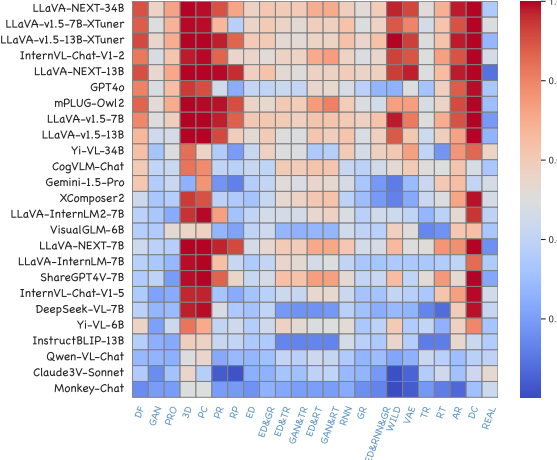


Figure 8. Results of Forensics-Bench from the perspective of *forgery model*. Current LVLMs still fell short in forgery detections across forgeries output by a wide range of forgery models.

els, we find that current LVLMs performed better on forgeries output by diffusion models (DF) compared with those output by GANs, which may expose the limited discerning capabilities of LVLMs for forgeries output by different AI models. Moreover, we find that current LVLMs experienced challenges when recognizing forgeries generated by the combinations of multiple AI models, such as Encoder-Decoder&Graphics-based methods (ED&GR), Generative Adversarial Networks&Transformer (GAN&TR) and etc. Such forgeries may pose more significant challenges to LVLMs’ forgery detection capabilities in the future.

4.3. Other Evaluation Protocol Analyses

Beyond the direct evaluations of Forensics-Bench, we further conduct *Robust Forgery Detection* and *Forgery Attribution* to complement the assessment of LVLMs’ forgery detection capabilities, providing more detailed analyses based on the comprehensive design of Forensics-Bench.

Protocol 1. Robust Forgery Detection. In this experiment, we mainly evaluated the performance of open-sourced top-performing LVLMs, including LLaVA-NEXT-34B, LLaVA-v1.5-7B-XTuner, InternVL-Chat-V1-2 and mPLUG-Owl2. Following previous studies [20, 31, 36], we reported the average overall score among 5 different intensity levels for each kind of perturbation. The results are summarized in Table 3. Intriguingly, we find that perturbations like change of color contrast and change of color saturation tended to compromised LVLMs’ abilities to perform forgery detections. Meanwhile, other perturbations, such as local block-wise distortion, had a less negative impact, which may even enhance LVLMs’ capabilities to distinguish forgeries. We argue that this is mostly because perturbations like local block-wise distortion would signif-

Model	Saturation	Contrast	Block	Noise	Blur	Pixel
LLaVA-NEXT-34B	62.3	61.2	68.8	67.0	62.0	63.2
LLaVA-v1.5-7B-XTuner	59.0	58.2	65.2	62.6	59.1	58.7
InternVL-Chat-V1-2	54.0	55.4	67.8	60.1	61.1	57.3
mPLUG-Owl2	55.5	55.8	64.4	60.2	62.3	58.0

Table 3. Robust forgery detection results for LVLMs across 6 perturbation types are summarized. The overall score is calculated across all data in Forensics-Bench.

Model	Overall	Semantic	Modality	Task	Type	Model
LLaVA-NEXT-34B	44.0	25.3	32.0	26.7	28.8	31.2
LLaVA-v1.5-7B-XTuner	42.2	31.4	42.3	32.6	32.2	33.3
InternVL-Chat-V1-2	41.6	24.4	30.9	26.3	29.8	31.1
mPLUG-Owl2	39.9	34.7	46.7	36.3	38.1	33.5

Table 4. Forgery attribution results for LVLMs across 5 perspectives of forgery detection are summarized. Accuracy is the metric.

icantly help reduce the content bias of forgeries, which is also experimentally verified to be effective for forgery detections in previous studies [20, 49, 96, 97].

Protocol 2. Forgery Attribution. In this experiment, we repurposed the forgery binary classification data in our benchmark into forgery attribution samples. For example, we asked LVLMs “*What is the forgery model that is applied to this RGB image?*”, along with 4 options sampled from our forgery models set. Similarly, we evaluated the performance of LLaVA-NEXT-34B, LLaVA-v1.5-7B-XTuner, InternVL-Chat-V1-2 and mPLUG-Owl2. The reported accuracy results are summarized in Table 4. We find that although these models demonstrated relatively great performance on forgery binary classification (c.f. Fig. 6), they encountered obstacles in performing fine-grained classification of different forgery models, highlighting the challenges of complex forgery detection scenarios.

5. Conclusion

In this paper, we have presented Forensics-Bench, a comprehensive benchmark designed to comprehensively assess LVLMs’ discerning capabilities on forgery media, evaluating recognition, location and reasoning capabilities on diverse forgeries. Through this comprehensive task design, our benchmark has provided thorough evaluations of the current popular LVLMs in the domain of forgery detection. Our experiments have effectively uncovered their weaknesses and biases in this field, offering valuable insights for future improvements in their performance on all-round forgery detection goals. We hope that our benchmark can serve as a platform for exploring the use of LVLMs in forgery detection tasks, potentially expanding the overall capability maps of LVLMs towards the next level of AGI.

Acknowledgements

This paper is partially supported by the National Key R&D Program of China No.2022ZD0161000 and the General Research Fund of Hong Kong No.17200622 and 17209324.

References

- [1] Anthropic. Claude, 2023. Accessed: 2023-04-18. [6, 7](#)
- [2] Jinze Bai, Shuai Bai, Shusheng Yang, Shijie Wang, Sinan Tan, Peng Wang, Junyang Lin, Chang Zhou, and Jingren Zhou. Qwen-vl: A frontier large vision-language model with versatile abilities. *arXiv preprint arXiv:2308.12966*, 2023. [1, 6, 7](#)
- [3] Chaitali Bhattacharyya, Hanxiao Wang, Feng Zhang, Sungho Kim, and Xiatian Zhu. Diffusion deepfake. *arXiv preprint arXiv:2404.01579*, 2024. [3](#)
- [4] Google AI Blog. Contributing data to deepfake detection research. <https://ai.googleblog.com/2019/09/contributing-data-to-deepfake-detection.html>, 2019. Accessed: 2021-11-13. [2](#)
- [5] Zhixi Cai, Shreya Ghosh, Aman Pankaj Adatia, Munawar Hayat, Abhinav Dhall, Tom Gedeon, and Kalin Stefanov. Av-deepfake1m: A large-scale llm-driven audio-visual deepfake dataset. *arXiv preprint arXiv:2311.15308*, 2023. [4](#)
- [6] You-Ming Chang, Chen Yeh, Wei-Chen Chiu, and Ning Yu. Antifakeprompt: Prompt-tuned vision-language models are fake image detectors, 2024. [1, 4](#)
- [7] Lin Chen, Jisong Li, Xiaoyi Dong, Pan Zhang, Conghui He, Jiaqi Wang, Feng Zhao, and Dahua Lin. Sharegpt4v: Improving large multi-modal models with better captions. *arXiv preprint arXiv:2311.12793*, 2023. [3, 6, 7](#)
- [8] Zhe Chen, Weiyun Wang, Hao Tian, Shenglong Ye, Zhangwei Gao, Erfei Cui, Wenwen Tong, Kongzhi Hu, Jiapeng Luo, Zheng Ma, et al. How far are we to gpt-4v? closing the gap to commercial multimodal models with open-source suites. *arXiv preprint arXiv:2404.16821*, 2024. [1, 6, 7](#)
- [9] Harry Cheng, Yangyang Guo, Tianyi Wang, Liqiang Nie, and Mohan Kankanhalli. Diffusion facial forgery detection. In *Proceedings of the 32nd ACM International Conference on Multimedia*, pages 5939–5948, 2024. [2, 3](#)
- [10] Sijie Cheng, Zhicheng Guo, Jingwen Wu, Kechen Fang, Peng Li, Huaping Liu, and Yang Liu. Can vision-language models think from a first-person perspective? *arXiv preprint arXiv:2311.15596*, 2023. [3](#)
- [11] Aakanksha Chowdhery, Sharan Narang, Jacob Devlin, Maarten Bosma, Gaurav Mishra, Adam Roberts, Paul Barham, Hyung Won Chung, Charles Sutton, Sebastian Gehrmann, et al. Palm: Scaling language modeling with pathways. *arXiv preprint arXiv:2204.02311*, 2022. [3](#)
- [12] OpenCompass Contributors. Opencompass: A universal evaluation platform for foundation models. <https://github.com/open-compass/opencompass>, 2023. [6, 7](#)
- [13] XTuner Contributors. Xtuner: A toolkit for efficiently fine-tuning llm. <https://github.com/InternLM/xtuner>, 2023. [6, 7](#)
- [14] Wenliang Dai, Junnan Li, Dongxu Li, Anthony Meng Huat Tiong, Junqi Zhao, Weisheng Wang, Boyang Li, Pascale Fung, and Steven Hoi. Instructblip: Towards general-purpose vision-language models with instruction tuning, 2023. [3, 6, 7](#)
- [15] Hao Dang, Feng Liu, Joel Stehouwer, Xiaoming Liu, and Anil K Jain. On the detection of digital face manipulation. In *Proceedings of the IEEE/CVF Conference on Computer Vision and Pattern recognition*, pages 5781–5790, 2020. [2, 3, 4](#)
- [16] Xinyi Ding, Zohreh Raziei, Eric C Larson, Eli V Olinick, Paul Krueger, and Michael Hahsler. Swapped face detection using deep learning and subjective assessment. *EURASIP Journal on Information Security*, 2020:1–12, 2020. [3](#)
- [17] B Dolhansky. The dee pfake detection challenge (dfdc) pre view dataset. *arXiv preprint arXiv:1910.08854*, 2019. [2, 6](#)
- [18] Brian Dolhansky, Joanna Bitton, Ben Pflaum, Jikuo Lu, Russ Howes, Menglin Wang, and Cristian Canton Ferrer. The deepfake detection challenge dataset. *arXiv e-prints*, pages arXiv–2006, 2020. [3, 4, 5](#)
- [19] Shichao Dong, Jin Wang, Jiajun Liang, Haoqiang Fan, and Renhe Ji. Explaining deepfake detection by analysing image matching. In *European conference on computer vision*, pages 18–35. Springer, 2022. [3](#)
- [20] Shichao Dong, Jin Wang, Renhe Ji, Jiajun Liang, Haoqiang Fan, and Zheng Ge. Implicit identity leakage: The stumbling block to improving deepfake detection generalization. In *Proceedings of the IEEE/CVF Conference on Computer Vision and Pattern Recognition (CVPR)*, pages 3994–4004, 2023. [1, 3, 8](#)
- [21] Xiaoyi Dong, Pan Zhang, Yuhang Zang, Yuhang Cao, Bin Wang, Linke Ouyang, Xilin Wei, Songyang Zhang, Haodong Duan, Maosong Cao, Wenwei Zhang, Yining Li, Hang Yan, Yang Gao, Xinyue Zhang, Wei Li, Jingwen Li, Kai Chen, Conghui He, Xingcheng Zhang, Yu Qiao, Dahua Lin, and Jiaqi Wang. Internlm-xcomposer2: Mastering free-form text-image composition and comprehension in vision-language large model. *arXiv preprint arXiv:2401.16420*, 2024. [3, 6, 7](#)
- [22] Haodong Duan, Junming Yang, Yuxuan Qiao, Xinyu Fang, Lin Chen, Yuan Liu, Xiaoyi Dong, Yuhang Zang, Pan Zhang, Jiaqi Wang, Dahua Lin, and Kai Chen. Vlmevalkit: An open-source toolkit for evaluating large multi-modality models, 2024. [6](#)
- [23] Patrick Esser, Robin Rombach, and Bjorn Ommer. Taming transformers for high-resolution image synthesis. In *Proceedings of the IEEE/CVF conference on computer vision and pattern recognition*, pages 12873–12883, 2021. [1, 3](#)
- [24] FaceSwapDevs. Deepfakes. <https://github.com/deepfakes/faceswap>, 2019. [1](#)
- [25] Chao Feng, Ziyang Chen, and Andrew Owens. Self-supervised video forensics by audio-visual anomaly detection. In *Proceedings of the IEEE/CVF Conference on Computer Vision and Pattern Recognition*, pages 10491–10503, 2023. [3](#)

[26] Chaoyou Fu, Peixian Chen, Yunhang Shen, Yulei Qin, Mengdan Zhang, Xu Lin, Zhenyu Qiu, Wei Lin, Jinrui Yang, Xiawu Zheng, Ke Li, Xing Sun, and Rongrong Ji. Mme: A comprehensive evaluation benchmark for multimodal large language models. *arXiv preprint arXiv:2306.13394*, 2023. 3

[27] Sharath Girish, Saksham Suri, Sai Saketh Rambhatla, and Abhinav Shrivastava. Towards discovery and attribution of open-world gan generated images. In *Proceedings of the IEEE/CVF International Conference on Computer Vision*, pages 14094–14103, 2021. 4, 6

[28] Ian Goodfellow, Jean Pouget-Abadie, Mehdi Mirza, Bing Xu, David Warde-Farley, Sherjil Ozair, Aaron Courville, and Yoshua Bengio. Generative adversarial nets. *Advances in neural information processing systems*, 27, 2014. 1, 3

[29] Yash Goyal, Tejas Khot, Douglas Summers-Stay, Dhruv Batra, and Devi Parikh. Making the v in vqa matter: Elevating the role of image understanding in visual question answering. In *Proceedings of the IEEE conference on computer vision and pattern recognition*, pages 6904–6913, 2017. 3

[30] Xiao Guo, Xiaohong Liu, Zhiyuan Ren, Steven Grosz, Iacopo Masi, and Xiaoming Liu. Hierarchical fine-grained image forgery detection and localization. In *Proceedings of the IEEE/CVF Conference on Computer Vision and Pattern Recognition*, pages 3155–3165, 2023. 1, 3, 2, 4

[31] Alexandros Haliassos, Konstantinos Vougioukas, Stavros Petridis, and Maja Pantic. Lips don't lie: A generalisable and robust approach to face forgery detection. In *Proceedings of the IEEE/CVF conference on computer vision and pattern recognition*, pages 5039–5049, 2021. 6, 8

[32] Yinan He, Bei Gan, Siyu Chen, Yichun Zhou, Guojun Yin, Luchuan Song, Lu Sheng, Jing Shao, and Ziwei Liu. Forgerynet: A versatile benchmark for comprehensive forgery analysis. In *Proceedings of the IEEE/CVF conference on computer vision and pattern recognition*, pages 4360–4369, 2021. 4, 2, 3, 5, 6

[33] Jonathan Ho, Ajay Jain, and Pieter Abbeel. Denoising diffusion probabilistic models. *Advances in neural information processing systems*, 33:6840–6851, 2020. 1, 3, 5

[34] Wenyi Hong, Ming Ding, Wendi Zheng, Xinghan Liu, and Jie Tang. Cogvideo: Large-scale pretraining for text-to-video generation via transformers. *arXiv preprint arXiv:2205.15868*, 2022. 2, 6

[35] Shan Jia, Reilin Lyu, Kangran Zhao, Yize Chen, Zhiyuan Yan, Yan Ju, Chuanbo Hu, Xin Li, Baoyuan Wu, and Siwei Lyu. Can chatgpt detect deepfakes? a study of using multimodal large language models for media forensics, 2024. 1, 4

[36] Liming Jiang, Ren Li, Wayne Wu, Chen Qian, and Chen Change Loy. Deepforensics-1.0: A large-scale dataset for real-world face forgery detection. In *Proceedings of the IEEE/CVF conference on computer vision and pattern recognition*, pages 2889–2898, 2020. 4, 6, 8, 2

[37] Ruihan Jin, Ruibo Fu, Zhengqi Wen, Shuai Zhang, Yukun Liu, and Jianhua Tao. Fake news detection and manipulation reasoning via large vision-language models, 2024. 1, 4

[38] Hasam Khalid, Shahroz Tariq, Minha Kim, and Simon S Woo. Fakeavceleb: A novel audio-video multimodal deepfake dataset. In *Thirty-fifth Conference on Neural Information Processing Systems Datasets and Benchmarks Track (Round 2)*, 2021. 4

[39] Pavel Korshunov and Sébastien Marcel. Deepfakes: a new threat to face recognition? assessment and detection. *arXiv preprint arXiv:1812.08685*, 2018. 2

[40] Marek Kowalski. FaceSwap. <https://github.com/MarekKowalski/FaceSwap>, 2018. 1

[41] PKU-Yuan Lab and Tuzhan AI etc. Open-sora-plan, 2024. 4, 2

[42] Trung-Nghia Le, Huy H Nguyen, Junichi Yamagishi, and Isao Echizen. Openforensics: Large-scale challenging dataset for multi-face forgery detection and segmentation in-the-wild. In *Proceedings of the IEEE/CVF international conference on computer vision*, pages 10117–10127, 2021. 4, 3

[43] Bohao Li, Rui Wang, Guangzhi Wang, Yuying Ge, Yixiao Ge, and Ying Shan. Seed-bench: Benchmarking multimodal llms with generative comprehension. *arXiv preprint arXiv:2307.16125*, 2023. 3

[44] Jiaming Li, Hongtao Xie, Jiahong Li, Zhongyuan Wang, and Yongdong Zhang. Frequency-aware discriminative feature learning supervised by single-center loss for face forgery detection. In *Proceedings of the IEEE/CVF Conference on Computer Vision and Pattern Recognition*, pages 6458–6467, 2021. 3

[45] Lingzhi Li, Jianmin Bao, Ting Zhang, Hao Yang, Dong Chen, Fang Wen, and Baining Guo. Face x-ray for more general face forgery detection. In *Proceedings of the IEEE/CVF Conference on Computer Vision and Pattern Recognition*, pages 5001–5010, 2020. 1, 3

[46] Yuezun Li, Xin Yang, Pu Sun, Honggang Qi, and Siwei Lyu. Celeb-df: A large-scale challenging dataset for deepfake forensics. In *Proceedings of the IEEE/CVF Conference on Computer Vision and Pattern Recognition*, pages 3207–3216, 2020. 3, 4, 5, 2

[47] Yixuan Li, Xuelin Liu, Xiaoyang Wang, Shiqi Wang, and Weisi Lin. Fakebench: Uncover the achilles' heels of fake images with large multimodal models. *arXiv preprint arXiv:2404.13306*, 2024. 1, 3, 4

[48] Zhang Li, Biao Yang, Qiang Liu, Zhiyin Ma, Shuo Zhang, Jingxu Yang, Yabo Sun, Yuliang Liu, and Xiang Bai. Monkey: Image resolution and text label are important things for large multi-modal models. In *proceedings of the IEEE/CVF conference on computer vision and pattern recognition*, 2024. 6, 7

[49] Jiahao Liang, Huafeng Shi, and Weihong Deng. Exploring disentangled content information for face forgery detection. In *European Conference on Computer Vision*, pages 128–145. Springer, 2022. 8

[50] Li Lin, Neeraj Gupta, Yue Zhang, Hainan Ren, Chun-Hao Liu, Feng Ding, Xin Wang, Xin Li, Luisa Verdoliva, and Shu Hu. Detecting multimedia generated by large ai models: A survey, 2024. 4

[51] Tsung-Yi Lin, Michael Maire, Serge Belongie, James Hays, Pietro Perona, Deva Ramanan, Piotr Dollár, and

C Lawrence Zitnick. Microsoft coco: Common objects in context. In *Computer Vision–ECCV 2014: 13th European Conference, Zurich, Switzerland, September 6–12, 2014, Proceedings, Part V 13*, pages 740–755. Springer, 2014. 4

[52] Haotian Liu, Chunyuan Li, Yuheng Li, and Yong Jae Lee. Improved baselines with visual instruction tuning, 2023. 3, 6, 7

[53] Haotian Liu, Chunyuan Li, Qingsong Wu, and Yong Jae Lee. Visual instruction tuning, 2023. 1, 3, 6, 7

[54] Haotian Liu, Chunyuan Li, Yuheng Li, Bo Li, Yuanhan Zhang, Sheng Shen, and Yong Jae Lee. Llava-next: Improved reasoning, ocr, and world knowledge, 2024. 6, 7

[55] Xuannan Liu, Pei Pei Li, Huaibo Huang, Zekun Li, Xing Cui, Weihong Deng, Zhaofeng He, et al. Fka-owl: Advancing multimodal fake news detection through knowledge-augmented l1vlms. In *ACM Multimedia 2024*, 2024. 1, 4

[56] Xuannan Liu, Zekun Li, Peipei Li, Shuhan Xia, Xing Cui, Linzhi Huang, Huaibo Huang, Weihong Deng, and Zhaofeng He. Mmfakebench: A mixed-source multimodal misinformation detection benchmark for l1vlms. *arXiv preprint arXiv:2406.08772*, 2024. 1, 3, 4

[57] Yuan Liu, Haodong Duan, Yuanhan Zhang, Bo Li, Songyang Zhang, Wangbo Zhao, Yike Yuan, Jiaqi Wang, Conghui He, Ziwei Liu, et al. Mmbench: Is your multimodal model an all-around player? *arXiv preprint arXiv:2307.06281*, 2023. 3

[58] Haoyu Lu, Wen Liu, Bo Zhang, Bingxuan Wang, Kai Dong, Bo Liu, Jingxiang Sun, Tongzheng Ren, Zhusu Li, Hao Yang, et al. Deepseek-vl: towards real-world vision-language understanding. *arXiv preprint arXiv:2403.05525*, 2024. 6, 7

[59] Zeyu Lu, Di Huang, Lei Bai, Jingjing Qu, Chengyue Wu, Xihui Liu, and Wanli Ouyang. Seeing is not always believing: benchmarking human and model perception of ai-generated images. *Advances in Neural Information Processing Systems*, 36, 2024. 2

[60] Grace Luo, Trevor Darrell, and Anna Rohrbach. Newsclipplings: Automatic generation of out-of-context multimodal media. *arXiv preprint arXiv:2104.05893*, 2021. 1, 3, 4

[61] Gen Luo, Yiyi Zhou, Tianhe Ren, Shengxin Chen, Xiaoshuai Sun, and Rongrong Ji. Cheap and quick: Efficient vision-language instruction tuning for large language models. *arXiv preprint arXiv:2305.15023*, 2023. 3

[62] Kenneth Marino, Mohammad Rastegari, Ali Farhadi, and Roozbeh Mottaghi. Ok-vqa: A visual question answering benchmark requiring external knowledge. In *Proceedings of the IEEE/cvf conference on computer vision and pattern recognition*, pages 3195–3204, 2019. 3

[63] Francesco Marra, Diego Gragnaniello, Davide Cozzolino, and Luisa Verdoliva. Detection of gan-generated fake images over social networks. In *2018 IEEE Conference on Multimedia Information Processing and Retrieval (MIPR)*, pages 384–389. IEEE, 2018. 3

[64] Fanqing Meng, Jin Wang, Chuanhao Li, Quanfeng Lu, Hao Tian, Jiaqi Liao, Xizhou Zhu, Jifeng Dai, Yu Qiao, Ping Luo, et al. Mmiu: Multimodal multi-image understanding for evaluating large vision-language models. *arXiv preprint arXiv:2408.02718*, 2024. 6

[65] Meredith Ringel Morris, Jascha Sohl-Dickstein, Noah Fiedel, Tris Warkentin, Allan Dafoe, Aleksandra Faust, Clement Farabet, and Shane Legg. Position: Levels of agi for operationalizing progress on the path to agi. In *Forty-first International Conference on Machine Learning*. 1

[66] Kartik Narayan, Harsh Agarwal, Kartik Thakral, Surbhi Mittal, Mayank Vatsa, and Richa Singh. Df-platter: Multi-face heterogeneous deepfake dataset. In *Proceedings of the IEEE/CVF Conference on Computer Vision and Pattern Recognition*, pages 9739–9748, 2023. 2

[67] Utkarsh Ojha, Yuheng Li, and Yong Jae Lee. Towards universal fake image detectors that generalize across generative models. In *Proceedings of the IEEE/CVF Conference on Computer Vision and Pattern Recognition*, pages 24480–24489, 2023. 4

[68] OpenAI. Chatgpt. <https://chat.openai.com/>, 2023. 3

[69] OpenAI. Gpt-4o. <https://openai.com/index/hello-gpt-4o/>, 2024. 1, 6, 7

[70] Long Ouyang, Jeffrey Wu, Xu Jiang, Diogo Almeida, Carroll Wainwright, Pamela Mishkin, Chong Zhang, Sandhini Agarwal, Katarina Slama, Alex Ray, et al. Training language models to follow instructions with human feedback. *Advances in Neural Information Processing Systems*, 35: 27730–27744, 2022. 3

[71] Dustin Podell, Zion English, Kyle Lacey, Andreas Blattmann, Tim Dockhorn, Jonas Müller, Joe Penna, and Robin Rombach. Sdxl: Improving latent diffusion models for high-resolution image synthesis. *arXiv preprint arXiv:2307.01952*, 2023. 4

[72] Peng Qi, Zehong Yan, Wynne Hsu, and Mong Li Lee. Sniffer: Multimodal large language model for explainable out-of-context misinformation detection. In *Proceedings of the IEEE/CVF Conference on Computer Vision and Pattern Recognition*, pages 13052–13062, 2024. 1, 4

[73] Alec Radford, Jong Wook Kim, Chris Hallacy, Aditya Ramesh, Gabriel Goh, Sandhini Agarwal, Girish Sastry, Amanda Askell, Pamela Mishkin, Jack Clark, et al. Learning transferable visual models from natural language supervision. In *International conference on machine learning*, pages 8748–8763. PMLR, 2021. 3

[74] Robin Rombach, Andreas Blattmann, Dominik Lorenz, Patrick Esser, and Björn Ommer. High-resolution image synthesis with latent diffusion models. In *Proceedings of the IEEE/CVF conference on computer vision and pattern recognition*, pages 10684–10695, 2022. 1, 4

[75] Andreas Rossler, Davide Cozzolino, Luisa Verdoliva, Christian Riess, Justus Thies, and Matthias Nießner. Faceforensics++: Learning to detect manipulated facial images. In *Proceedings of the IEEE/CVF International Conference on Computer Vision*, pages 1–11, 2019. 3, 4, 5, 2

[76] Conrad Sanderson and Brian C Lovell. Multi-region probabilistic histograms for robust and scalable identity inference. In *Advances in biometrics: Third international conference, ICB 2009, alghero, italy, june 2–5, 2009. Proceedings 3*, pages 199–208. Springer, 2009. 2

[77] Dustin Schwenk, Apoorv Khandelwal, Christopher Clark, Kenneth Marino, and Roozbeh Mottaghi. A-okvqa: A

benchmark for visual question answering using world knowledge. In *European Conference on Computer Vision*, pages 146–162. Springer, 2022. 3

[78] Rui Shao, Tianxing Wu, and Ziwei Liu. Detecting and grounding multi-modal media manipulation. In *Proceedings of the IEEE/CVF Conference on Computer Vision and Pattern Recognition*, pages 6904–6913, 2023. 1, 3, 4, 7, 5, 6

[79] Piyush Sharma, Nan Ding, Sebastian Goodman, and Radu Soricut. Conceptual captions: A cleaned, hypernymed, image alt-text dataset for automatic image captioning. In *Proceedings of the 56th Annual Meeting of the Association for Computational Linguistics (Volume 1: Long Papers)*, pages 2556–2565, 2018. 3

[80] Yichen Shi, Yuhao Gao, Yingxin Lai, Hongyang Wang, Jun Feng, Lei He, Jun Wan, Changsheng Chen, Zitong Yu, and Xiaochun Cao. Shield: An evaluation benchmark for face spoofing and forgery detection with multimodal large language models. *arXiv preprint arXiv:2402.04178*, 2024. 1, 4

[81] Kaede Shiohara and Toshihiko Yamasaki. Detecting deepfakes with self-blended images. In *Proceedings of the IEEE/CVF Conference on Computer Vision and Pattern Recognition*, pages 18720–18729, 2022. 1, 3

[82] Zekun Sun, Yujie Han, Zeyu Hua, Na Ruan, and Weijia Jia. Improving the efficiency and robustness of deepfakes detection through precise geometric features. In *Proceedings of the IEEE/CVF Conference on Computer Vision and Pattern Recognition*, pages 3609–3618, 2021. 3

[83] Shahroz Tariq, Sangyup Lee, Hoyoung Kim, Youjin Shin, and Simon S Woo. Detecting both machine and human created fake face images in the wild. In *Proceedings of the 2nd international workshop on multimedia privacy and security*, pages 81–87, 2018. 3

[84] Gemini Team. Gemini: A family of highly capable multimodal models, 2023. 1, 7

[85] Gemini Team, Petko Georgiev, Ving Ian Lei, Ryan Burnell, Libin Bai, Anmol Gulati, Garrett Tanzer, Damien Vincent, Zhufeng Pan, Shibo Wang, et al. Gemini 1.5: Unlocking multimodal understanding across millions of tokens of context. *arXiv preprint arXiv:2403.05530*, 2024. 6

[86] InternLM Team. Internlm: A multilingual language model with progressively enhanced capabilities. <https://github.com/InternLM/InternLM-technote>, 2023. 3, 6, 7

[87] Hugo Touvron, Louis Martin, Kevin Stone, Peter Albert, Amjad Almahairi, Yasmine Babaei, Nikolay Bashlykov, Soumya Batra, Prajjwal Bhargava, Shruti Bhosale, et al. Llama 2: Open foundation and fine-tuned chat models, 2023. 3

[88] Shengkang Wang, Hongzhan Lin, Ziyang Luo, Zhen Ye, Guang Chen, and Jing Ma. Mfc-bench: Benchmarking multimodal fact-checking with large vision-language models. *arXiv preprint arXiv:2406.11288*, 2024. 1, 3, 4

[89] Sheng-Yu Wang, Oliver Wang, Richard Zhang, Andrew Owens, and Alexei A Efros. Cnn-generated images are surprisingly easy to spot... for now. In *Proceedings of the IEEE/CVF conference on computer vision and pattern recognition*, pages 8695–8704, 2020. 4, 2, 3, 5

[90] Weihan Wang, Qingsong Lv, Wenmeng Yu, Wenyi Hong, Ji Qi, Yan Wang, Junhui Ji, Zhuoyi Yang, Lei Zhao, Xixuan Song, Jiazheng Xu, Bin Xu, Juanzi Li, Yuxiao Dong, Ming Ding, and Jie Tang. Cogvilm: Visual expert for pretrained language models. 2023. 6, 7

[91] Yukai Wang, Chunlei Peng, Decheng Liu, Nannan Wang, and Xinbo Gao. Forgernir: deep face forgery and detection in near-infrared scenario. *Ieee transactions on information forensics and security*, 17:500–515, 2022. 4, 2, 3

[92] Zhendong Wang, Jianmin Bao, Wengang Zhou, Weilun Wang, Hezhen Hu, Hong Chen, and Houqiang Li. Dire for diffusion-generated image detection. In *Proceedings of the IEEE/CVF International Conference on Computer Vision*, pages 22445–22455, 2023. 4, 2, 5

[93] Guangyang Wu, Weijie Wu, Xiaohong Liu, Kele Xu, Tianjiao Wan, and Wenyi Wang. Cheap-fake detection with llm using prompt engineering, 2023. 4

[94] Haoning Wu, Zicheng Zhang, Erli Zhang, Chaofeng Chen, Liang Liao, Annan Wang, Chunyi Li, Wenxiu Sun, Qiong Yan, Guangtao Zhai, et al. Q-bench: A benchmark for general-purpose foundation models on low-level vision. *arXiv preprint arXiv:2309.14181*, 2023. 3

[95] Zhiyuan Yan, Taiping Yao, Shen Chen, Yandan Zhao, Xinghe Fu, Junwei Zhu, Donghao Luo, Chengjie Wang, Shouhong Ding, Yunsheng Wu, et al. Df40: Toward next-generation deepfake detection. In *The Thirty-eighth Conference on Neural Information Processing Systems Datasets and Benchmarks Track*. 3

[96] Zhiyuan Yan, Yong Zhang, Yanbo Fan, and Baoyuan Wu. Ucf: Uncovering common features for generalizable deepfake detection. In *Proceedings of the IEEE/CVF International Conference on Computer Vision*, pages 22412–22423, 2023. 3, 8

[97] Zhiyuan Yan, Yuhao Luo, Siwei Lyu, Qingshan Liu, and Baoyuan Wu. Transcending forgery specificity with latent space augmentation for generalizable deepfake detection. In *Proceedings of the IEEE/CVF Conference on Computer Vision and Pattern Recognition*, pages 8984–8994, 2024. 3, 8

[98] Aiyuan Yang, Bin Xiao, Bingning Wang, Borong Zhang, Ce Bian, Chao Yin, Chenxu Lv, Da Pan, Dian Wang, Dong Yan, et al. Baichuan 2: Open large-scale language models, 2023. 3

[99] Tianyun Yang, Ziyao Huang, Juan Cao, Lei Li, and Xirong Li. Deepfake network architecture attribution. In *Proceedings of the AAAI Conference on Artificial Intelligence*, pages 4662–4670, 2022. 4, 6

[100] Zhuoyi Yang, Jiayan Teng, Wendi Zheng, Ming Ding, Shiyu Huang, Jiazheng Xu, Yuanming Yang, Wenyi Hong, Xiaohan Zhang, Guanyu Feng, et al. Cogvideox: Text-to-video diffusion models with an expert transformer. *arXiv preprint arXiv:2408.06072*, 2024. 3, 4

[101] Qinghao Ye, Haiyang Xu, Jiabo Ye, Ming Yan, Anwen Hu, Haowei Liu, Qi Qian, Ji Zhang, and Fei Huang. mplug-owl2: Revolutionizing multi-modal large language

model with modality collaboration. In *Proceedings of the IEEE/CVF Conference on Computer Vision and Pattern Recognition*, pages 13040–13051, 2024. 3, 6, 7

[102] Kaining Ying, Fanqing Meng, Jin Wang, Zhiqian Li, Han Lin, Yue Yang, Hao Zhang, Wenbo Zhang, Yuqi Lin, Shuo Liu, et al. Mmt-bench: A comprehensive multimodal benchmark for evaluating large vision-language models towards multitask agi, 2024. 3, 6

[103] Alex Young, Bei Chen, Chao Li, Chengan Huang, Ge Zhang, Guanwei Zhang, Heng Li, Jiangcheng Zhu, Jianqun Chen, Jing Chang, et al. Yi: Open foundation models by 01. ai. *arXiv preprint arXiv:2403.04652*, 2024. 6, 7

[104] Weihao Yu, Zhengyuan Yang, Linjie Li, Jianfeng Wang, Kevin Lin, Zicheng Liu, Xinchao Wang, and Lijuan Wang. Mm-vet: Evaluating large multimodal models for integrated capabilities. *arXiv preprint arXiv:2308.02490*, 2023. 3

[105] Xiang Yue, Yuansheng Ni, Kai Zhang, Tianyu Zheng, Ruqi Liu, Ge Zhang, Samuel Stevens, Dongfu Jiang, Weiming Ren, Yuxuan Sun, et al. Mmmu: A massive multi-discipline multimodal understanding and reasoning benchmark for expert agi. *arXiv preprint arXiv:2311.16502*, 2023. 3, 6

[106] Rowan Zellers, Ari Holtzman, Hannah Rashkin, Yonatan Bisk, Ali Farhadi, Franziska Roesner, and Yejin Choi. Defending against neural fake news. *Advances in neural information processing systems*, 32, 2019. 4

[107] Pan Zhang, Xiaoyi Dong, Bin Wang, Yuhang Cao, Chao Xu, Linke Ouyang, Zhiyuan Zhao, Shuangrui Ding, Songyang Zhang, Haodong Duan, Wenwei Zhang, Hang Yan, Xinyue Zhang, Wei Li, Jingwen Li, Kai Chen, Conghui He, Xingcheng Zhang, Yu Qiao, Dahua Lin, and Jiaqi Wang. Internlm-xcomposer: A vision-language large model for advanced text-image comprehension and composition. *arXiv preprint arXiv:2309.15112*, 2023. 1

[108] Renrui Zhang, Jiaming Han, Chris Liu, Peng Gao, Ao-jun Zhou, Xiangfei Hu, Shilin Yan, Pan Lu, Hongsheng Li, and Yu Qiao. Llama-adapter: Efficient fine-tuning of language models with zero-init attention. *arXiv preprint arXiv:2303.16199*, 2023. 1

[109] Yuanhan Zhang, ZhenFei Yin, Yidong Li, Guojun Yin, Junjie Yan, Jing Shao, and Ziwei Liu. Celeba-spoof: Large-scale face anti-spoofing dataset with rich annotations. In *Computer Vision–ECCV 2020: 16th European Conference, Glasgow, UK, August 23–28, 2020, Proceedings, Part XII 16*, pages 70–85. Springer, 2020. 3, 4, 5

[110] Yue Zhang, Ben Colman, Xiao Guo, Ali Shahriyari, and Gaurav Bharaj. Common sense reasoning for deepfake detection. In *European Conference on Computer Vision*, pages 399–415. Springer, 2024. 1

[111] Hanqing Zhao, Wenbo Zhou, Dongdong Chen, Tianyi Wei, Weiming Zhang, and Nenghai Yu. Multi-attentional deepfake detection. In *Proceedings of the IEEE/CVF Conference on Computer Vision and Pattern Recognition*, pages 2185–2194, 2021. 3

[112] Tianchen Zhao, Xiang Xu, Mingze Xu, Hui Ding, Yuanjun Xiong, and Wei Xia. Learning self-consistency for deepfake detection. In *Proceedings of the IEEE/CVF international conference on computer vision*, pages 15023–15033, 2021. 1, 3

[113] Haokun Zhou and Yipeng Hong. Diffusyn bench: Evaluating vision-language models on real-world complexities with diffusion-generated synthetic benchmarks. *arXiv preprint arXiv:2406.04470*, 2024. 1, 4

[114] Tianfei Zhou, Wenguan Wang, Zhiyuan Liang, and Jianbing Shen. Face forensics in the wild. In *Proceedings of the IEEE/CVF conference on computer vision and pattern recognition*, pages 5778–5788, 2021. 2, 4, 6

[115] Deyao Zhu, Jun Chen, Xiaoqian Shen, Xiang Li, and Mohamed Elhoseiny. Minigpt-4: Enhancing vision-language understanding with advanced large language models. *arXiv preprint arXiv:2304.10592*, 2023. 3

[116] Mingjian Zhu, Hanting Chen, Qiangyu Yan, Xudong Huang, Guanyu Lin, Wei Li, Zhijun Tu, Hailin Hu, Jie Hu, and Yunhe Wang. Genimage: A million-scale benchmark for detecting ai-generated image. *Advances in Neural Information Processing Systems*, 36, 2024. 2, 5

[117] Bojia Zi, Minghao Chang, Jingjing Chen, Xingjun Ma, and Yu-Gang Jiang. Wilddeepfake: A challenging real-world dataset for deepfake detection. In *Proceedings of the 28th ACM international conference on multimedia*, pages 2382–2390, 2020. 2

Forensics-Bench: A Comprehensive Forgery Detection Benchmark Suite for Large Vision Language Models

Supplementary Material

6. Abbreviations for Forensics-Bench

The detailed abbreviations utilized throughout the paper are listed in Table 5.

Abbreviation	Full Term	Abbreviation	Full Term
Forgery Semantics			
HS	Human Subject	GS	General Subject
Forgery Modalities			
RGB	RGB Images	NIR	Near-infrared Images
VID	Videos	RGB&TXT	RGB Images and Texts
Forgery Tasks			
BC	Forgery Binary Classification	SLD	Forgery Spatial Localization (Detection)
SLS	Forgery Spatial Localization (Segmentation)	TL	Forgery Temporal Localization
Forgery Types			
ES	Entire Synthesis	SPF	Spoofing
FE	Face Editing	FE&FT	Face Editing & Face Transfer
FE&TAM	Face Editing & Text Attribute Manipulation	FE&TS	Face Editing & Text Swap
FR	Face Reenactment	FSM	Face Swap (Multiple Faces)
FSS	Face Swap (Single Face)	FSS&FE	Face Swap (Single Face) & Face Editing
FSS&TAM	Face Swap (Single Face) & Text Attribute Manipulation	FSS&TS	Face Swap (Single Face) & Text Swap
FT	Face Transfer	CM	Copy-Move
RM	Removal	SPL	Splicing
IE	Image Enhancement	REAL	Real media without being forged
OOC	Out-of-Context	ST	Style Translation
TAM	Text Attribute Manipulation	TS	Text Swap
Forgery Models			
3D	3D masks	RNN	Recurrent Neural Networks
TR	Transformer	DC	Decoder
DF	Diffusion models	ED	Encoder-Decoder
ED&RNN&GR	Encoder-Decoder&Recurrent Neural Networks&Graphics-based methods	ED&TR	Encoder-Decoder&Transformer
ED&RT	Encoder-Decoder&Retrieval-based methods	ED&GR	Encoder-Decoder&Graphics-based methods
GAN	Generative Adversarial Networks	GAN&TR	Generative Adversarial Networks&Transformer
GAN&RT	Generative Adversarial Networks&Retrieval-based methods	PC	Paper-Cut
Real	Real media without being forged	PR	Print
PRO	Proprietary	RP	Replay
RT	Retrieval-based methods	AR	Auto-regressive models
GR	Graphics-based methods	WILD	Unknown (in the wild)
VAE	Variational Auto-Encoders		

Table 5. The abbreviations of terms mentioned in Forensics-Bench and their corresponding full terms.

7. Data Structure of Forensics-Bench

In Table 6, Table 7 and Table 8, we present all 112 unique forgery detection types from Forensics-Bench, covering 5 designed perspectives characterizing forgeries. These tables include details on sample number, the specific information of 5 designed perspectives in Forensics-Bench and data sources collected under licenses.

8. Other Details of Forensics-Bench

Uniformed metadata. In our benchmark, we design a uniformed metadata structure to standardize and accelerate the construction process of our data samples. As shown in Table 9, the metadata structure is a dictionary with keys divided into three main categories. The first category contains keys such as the image path, image resolution and data source, describing the vanilla information about the raw data. The second category includes keys demonstrating the detailed information of 5 designed perspectives in our benchmark. The third category includes keys for the transformed Q&A, such as the question template, answer (ground truth) and choice list.

Forgery Task	Forgery Semantic	Forgery Type	Forgery Model	Forgery Modality	Data Sources	Sample Number
Forgery Binary Classification	Human Subject	Entire Synthesis	Generative Adversarial Networks	RGB Images	HiFi-IFDL(StyleGAN2-ada on FFHQ) [30]; HiFi-IFDL(StyleGAN3 on FFHQ) [30]; DFFD(ProGAN) [15]; DFFD(StyleGANv1) [15]; ForgeryNet(StyleGANv2) [32]; ForgeryNet(DiscoFaceGAN) [32]; Fake2M(StyleGANv3 on FFHQ/metface) [59]	2000
Forgery Binary Classification	Human Subject	Entire Synthesis	Generative Adversarial Networks	Near-infrared Images	ForgeryNIR(ProGAN) [91]; ForgeryNIR(StyleGAN) [91]; ForgeryNIR(StyleGAN2) [91]	1200
Forgery Binary Classification	General Subject	Entire Synthesis	Generative Adversarial Networks	RGB Images	HiFi-IFDL(StyleGAN2-ada on AFHQ) [30]; HiFi-IFDL(styleGAN3 on AFHQ) [30]; GenImage(BigGAN ImageNet classes) [116]; CNN-spot(ProGAN on LSUN) [89]; CNN-spot(StyleGAN1/v2 on LSUN) [89]; CNN-spot(BigGAN on ImageNet) [89]; Fake2M(StyleGAN3 on AFHQ) [59]	6000
Forgery Binary Classification	Human Subject	Entire Synthesis	Proprietary	RGB Images	Diff(midjourney) [9]; Diff(SDXL) [9]; Diff(FreeDoM.T) [9]; Diff(HPS) [9]; Diff(LoRA) [9]; Diff(DreamBooth) [9]; Diff(SDXL Refiner) [9]; Diff(FreeDoM.J) [9]	200
Forgery Binary Classification	Human Subject	Entire Synthesis	Diffusion models	RGB Images	Diff(midjourney) [9]; Diff(SDXL) [9]; Diff(FreeDoM.T) [9]; Diff(HPS) [9]; Diff(LoRA) [9]; Diff(DreamBooth) [9]; Diff(SDXL Refiner) [9]; Diff(FreeDoM.J) [9]	1400
Forgery Binary Classification	General Subject	Entire Synthesis	Diffusion models	Videos	Open-Sora-Plan [41]	100
Forgery Binary Classification	General Subject	Entire Synthesis	Auto-regressive models	Videos	Cogview [34]	100
Forgery Binary Classification	General Subject	Entire Synthesis	Diffusion models	RGB Images	HiFi-IFDL(GDM on LSUN) [30]; HiFi-IFDL(LDM on LSUN) [30]; HiFi-IFDL(DDPM on LSUN) [30]; HiFi-IFDL(DDIM on LSUN) [30]; GenImage(SD V1.4 on ImageNet classes) [116]; GenImage(SD V1.5 on ImageNet classes) [116]; GenImage(ADM on ImageNet classes) [116]; GenImage(GLIDE on ImageNet classes) [116]; Fake2M(SD V2.1) [59]; Fake2M(SD V1.5) [59]; Fake2M(IF V1.0) [59]; DiffusionForensics(ADM on LSUN) [92]; DiffusionForensics(DDPM on LSUN) [92]; DiffusionForensics(DDPM on LSUN) [92]; DiffusionForensics(PNDM on LSUN) [92]; DiffusionForensics(LDM on LSUN) [92]; DiffusionForensics(SD-v1 on LSUN) [92]; DiffusionForensics(SD-v2 on LSUN) [92]; DiffusionForensics(ADM on ImageNet) [92]; DiffusionForensics(SD-v1 on ImageNet) [92]	5800
Forgery Binary Classification	General Subject	Entire Synthesis	Proprietary	RGB Images	GenImage(Midjourney on ImageNet classes) [116]; GenImage(Wukong on ImageNet classes) [116]; Fake2M(Midjourney crawled in the website) [59]	600
Forgery Binary Classification	General Subject	Entire Synthesis	Variational Auto-Encoders	RGB Images	GenImage(VQDM on ImageNet classes) [116]; DiffusionForensics(VQ-Diffusion on LSUN) [92]	400
Forgery Binary Classification	General Subject	Entire Synthesis	Auto-regressive models	RGB Images	Fake2M(Cogview) [59]	200
Forgery Binary Classification	Human Subject	Face Swap (Single Face)	Graphics-based methods	Videos	FF++(FaceSwap) [75]	140
Forgery Binary Classification	Human Subject	Face Swap (Single Face)	Graphics-based methods	RGB Images	FF++(FaceSwap) [75]	200
Forgery Binary Classification	Human Subject	Face Swap (Single Face)	Encoder-Decoder	Videos	FF++(FaceShifter) [75]; FF++(Deepfakes) [75]; ForgeryNet(DeepFaceLab) [32]; ForgeryNet(FaceShifter) [32]; CelebDF-v2(Improved Deepfakes) [46]; DF-TIMIT(Improved Deepfakes) [39, 76]	1280
Forgery Binary Classification	Human Subject	Face Swap (Single Face)	Encoder-Decoder	RGB Images	FF++(FaceShifter) [75]; FF++(Deepfakes) [75]; ForgeryNet(DeepFaceLab) [32]; ForgeryNet(FaceShifter) [32]; CelebDF-v2(Improved Deepfakes) [46]; DF-TIMIT(Improved Deepfakes) [39, 76]	1400
Forgery Binary Classification	Human Subject	Face Swap (Single Face)	Variational Auto-Encoders	Videos	DeeperForensics(DeepFake VAE) [36]	200
Forgery Binary Classification	Human Subject	Face Swap (Single Face)	Variational Auto-Encoders	RGB Images	DeeperForensics(DeepFake VAE) [36]	200
Forgery Binary Classification	Human Subject	Face Swap (Single Face)	Recurrent Neural Networks	Videos	ForgeryNet(FSGAN) [32];	200
Forgery Binary Classification	Human Subject	Face Swap (Single Face)	Recurrent Neural Networks	RGB Images	ForgeryNet(FSGAN) [32];	200
Forgery Binary Classification	Human Subject	Face Swap (Single Face)	Unknown (in the wild)	Videos	DFDCP [17]; WildDeepfake [117]; DFD [4]	400
Forgery Binary Classification	Human Subject	Face Swap (Single Face)	Unknown (in the wild)	RGB Images	DFDCP [17]; WildDeepfake [117]; DFD [4]	400
Forgery Binary Classification	Human Subject	Face Swap (Single Face)	Diffusion models	RGB Images	Diff(DiffFace) [9]; Diff(DCFace) [9]	400
Forgery Binary Classification	Human Subject	Face Swap (Multiple Faces)	Encoder-Decoder, Recurrent Neural Networks, Graphics-based methods	Videos	FFIW(DeepFaceLab, FSGAN, FaceSwap) [114]; DF-Platter(FaceShifter) [66]	200
Forgery Binary Classification	Human Subject	Face Swap (Multiple Faces)	Encoder-Decoder, Recurrent Neural Networks, Graphics-based methods	RGB Images	FFIW(DeepFaceLab, FSGAN, FaceSwap) [114]; DF-Platter(FaceShifter) [66]	200
Forgery Binary Classification	Human Subject	Face Transfer	Graphics-based methods	Videos	ForgeryNet(BlendFace) [32]; ForgeryNet(MMReplacement) [32]	300
Forgery Binary Classification	Human Subject	Face Transfer	Graphics-based methods	RGB Images	ForgeryNet(BlendFace) [32]; ForgeryNet(MMReplacement) [32]	400
Forgery Binary Classification	Human Subject	Face Reenactment	Graphics-based methods	Videos	FF++(Face2Face) [75]	140
Forgery Binary Classification	Human Subject	Face Reenactment	Graphics-based methods	RGB Images	FF++(Face2Face) [75]	200
Forgery Binary Classification	Human Subject	Face Reenactment	Encoder-Decoder	Videos	FF++(NeuralTextures) [75]	140

Table 6. Forensics-Bench data structure (part 1): including the detailed information of 5 designed perspectives characterizing forgeries, sample number and data sources collected under licenses.

Details of forgery types. In our benchmark, we roughly classify previous forgeries into 21 types, which are summarized as follows.

- Entire Synthesis: In our benchmark, this refers to forgeries that are synthesized from scratch without a basis on real media. For instance, vanilla GAN models and diffusion models can generate forgeries from random Gaussian noises. Representative datasets of this type include CNN-spot [89] and DiffusionForensics [92].

Forgery Task	Forgery Semantic	Forgery Type	Forgery Model	Forgery Modality	Data Sources	Sample Number
Forgery Binary Classification	Human Subject	Face Reenactment	Encoder-Decoder	RGB Images	FF++(NeuralTextures) [75]; ForgeryNet(FirstOrderMotion) [32]	400
Forgery Binary Classification	Human Subject	Face Reenactment	Recurrent Neural Networks	Videos	ForgeryNet(ATVG-Net) [32]; ForgeryNet(Talking-head Video) [32]	400
Forgery Binary Classification	Human Subject	Face Reenactment	Recurrent Neural Networks	RGB Images	ForgeryNet(ATVG-Net) [32]; ForgeryNet(Talking-head Video) [32]	400
					HiFi-IFDL(starGANv2 on CelebHQ) [30]; HiFi-IFDL(HSD on CelebHQ) [30]; HiFi-IFDL(STGAN on CelebHQ) [30]; DFFD(starGAN on CelebA) [15]; ForgeryNet(starGANv2) [32]; ForgeryNet(MaskGAN) [32]; ForgeryNet(SC-FEGAN) [32]; CNN-spot(starGAN) [89]	
Forgery Binary Classification	Human Subject	Face Editing	Encoder-Decoder	RGB Images	DFFD(FaceAPP on FFHQ) [15]	1400
Forgery Binary Classification	Human Subject	Style Translation	Encoder-Decoder	Near-infrared Images	ForgeryNIR(CycleGAN) [91]	400
Forgery Binary Classification	Human Subject	Face Editing	Proprietary	RGB Images	Diffi(FaceAPP on FFHQ) [15]	200
Forgery Binary Classification	Human Subject	Face Editing	Diffusion models	RGB Images	Diff(Imagic) [9]; Diffi(CoDiff) [9]; Diffi(CycleDiff) [9]	600
Forgery Binary Classification	General Subject	Style Translation	Encoder-Decoder	RGB Images	CNN-spot(CycleGAN) [89]; CNN-spot(GauGAN) [89]	1260
Forgery Binary Classification	General Subject	Style Translation	Decoder	RGB Images	CNN-spot(CRN) [89]; CNN-spot(IME) [89]	400
Forgery Binary Classification	General Subject	Image Enhancement	Encoder-Decoder	RGB Images	CNN-spot(SITD) [89]; CNN-spot(SAN) [89]	380
Forgery Binary Classification	Human Subject	Face Editing/Face Transfer	Encoder-Decoder,Graphics-based methods	RGB Images	ForgeryNet(StarGAN2+BlendFace) [32]	200
Forgery Binary Classification	Human Subject	Face Swap (Single Face),Face Editing	Encoder-Decoder	Videos	ForgeryNet(DeepFaceLab-StarGAN) [32]	200
Forgery Binary Classification	Human Subject	Face Swap (Single Face),Face Editing	Encoder-Decoder	RGB Images	ForgeryNet(DeepFaceLab-StarGAN) [32]	200
Forgery Binary Classification	General Subject	Copy&Move	Graphics-based methods	RGB Images	HiFi-IFDL(PSCC-Net) [30]	200
Forgery Binary Classification	General Subject	Removal	Encoder-Decoder	RGB Images	HiFi-IFDL(PSCC-Net) [30]	200
Forgery Binary Classification	General Subject	Splicing	Graphics-based methods	RGB Images	HiFi-IFDL(PSCC-Net) [30]	200
Forgery Binary Classification	Human Subject	Face Swap (Single Face)	Encoder-Decoder	RGB Images,Texts	DGM4(SimSwap) [78]; DGM4(InfoSwap) [78]	400
Forgery Binary Classification	Human Subject	Face Editing	Encoder-Decoder	RGB Images,Texts	DGM4(HFGI) [78]	200
Forgery Binary Classification	Human Subject	Face Editing	Generative Adversarial Networks	RGB Images,Texts	DGM4(StyleCLIP) [78]	200
Forgery Binary Classification	Human Subject	Text Swap	Retrieval-based methods	RGB Images,Texts	DGM4(retrieval) [78]	200
Forgery Binary Classification	Human Subject	Text Attribute Manipulation	Transformer	RGB Images,Texts	DGM4(B-GST) [78]	200
Forgery Binary Classification	Human Subject	Face Swap (Single Face),Text Swap	Encoder-Decoder,Retrieval-based methods	RGB Images,Texts	DGM4(SimSwap+retrieval) [78]; DGM4(InfoSwap+retrieval) [78]	400
Forgery Binary Classification	Human Subject	Face Editing,Text Swap	Encoder-Decoder,Retrieval-based methods	RGB Images,Texts	DGM4(HFGI+retrieval) [78]	200
Forgery Binary Classification	Human Subject	Face Editing,Text Swap	Generative Adversarial Networks,Retrieval-based methods	RGB Images,Texts	DGM4(StyleCLIP+retrieval) [78]	200
Forgery Binary Classification	Human Subject	Face Swap (Single Face),Text Attribute Manipulation	Encoder-Decoder,Transformer	RGB Images,Texts	DGM4(SimSwap+B-GST) [78]; DGM4(InfoSwap+B-GST) [78]	400
Forgery Binary Classification	Human Subject	Face Editing,Text Attribute Manipulation	Encoder-Decoder,Transformer	RGB Images,Texts	DGM4(HFGI+B-GST) [78]	200
Forgery Binary Classification	Human Subject	Face Editing,Text Attribute Manipulation	Generative Adversarial Networks,Transformer	RGB Images,Texts	DGM4(StyleCLIP+B-GST) [78]	200
Forgery Binary Classification	Human Subject	Out-of-Context	Retrieval-based methods	RGB Images,Texts	NewCLIP-Spoof [60]	100
Forgery Binary Classification	Human Subject	Face Spoofing	Print	RGB Images	CelebA-Spoof [109]	200
Forgery Binary Classification	Human Subject	Face Spoofing	Paper Cut	RGB Images	CelebA-Spoof [109]	200
Forgery Binary Classification	Human Subject	Face Spoofing	Replay	RGB Images	CelebA-Spoof [109]	200
Forgery Binary Classification	Human Subject	Face Spoofing	3D masks	RGB Images	CelebA-Spoof [109]	200
Forgery Spatial Localization (Segmentation)	Human Subject	Face Swap (Single Face)	Encoder-Decoder	Videos	HiFi-IFDL(FaceShifter on Youtube video) [30]; DFFD(DeepFaceLab) [15]; DFFD(Deepfakes) [15]; ForgeryNet(FaceShifter) [32]; ForgeryNet(DeepFaceLab) [32]	309
Forgery Spatial Localization (Segmentation)	Human Subject	Face Swap (Single Face)	Encoder-Decoder	RGB Images	HiFi-IFDL(FaceShifter on Youtube video) [30]; DFFD(DeepFaceLab) [15]; DFFD(Deepfakes) [15]; ForgeryNet(FaceShifter) [32]; ForgeryNet(DeepFaceLab) [32]	598
Forgery Spatial Localization (Segmentation)	Human Subject	Face Swap (Single Face)	Graphics-based methods	Videos	FF++(FaceSwap) [75]	140
Forgery Spatial Localization (Segmentation)	Human Subject	Face Swap (Single Face)	Graphics-based methods	RGB Images	FF++(FaceSwap) [75]	200
Forgery Spatial Localization (Segmentation)	Human Subject	Face Swap (Single Face)	Recurrent Neural Networks	RGB Images	ForgeryNet(FSGAN) [32]	200
Forgery Spatial Localization (Segmentation)	Human Subject	Face Transfer	Graphics-based methods	Videos	ForgeryNet(BlandFace) [32]; ForgeryNet(MMRreplacement) [32]	231
Forgery Spatial Localization (Segmentation)	Human Subject	Face Transfer	Graphics-based methods	RGB Images	ForgeryNet(BlandFace) [32]; ForgeryNet(MMRreplacement) [32]	400
Forgery Spatial Localization (Segmentation)	Human Subject	Face Reenactment	Graphics-based methods	Videos	FF++(Face2Face) [75]	140

Table 7. Forensics-Bench data structure (part 2): including the detailed information of 5 designed perspectives characterizing forgeries, sample number and data sources collected under licenses.

- **Spoofing:** In our benchmark, this refers to forgeries that present a fake version of a legitimate user’s face to bypass authentication, such as the printed photograph of a user’s face, a recorded video of the target user and 3D masks that mimic the target’s facial structures. Representative datasets of this type include CelebA-Spoof [109].
- **Face Editing:** In our benchmark, this refers to forgeries that modify the external attributes of human faces, such as facial hair, age and gender. Representative datasets of this type include ForgeryNet [32].
- **Face Swap (Single Face):** In our benchmark, this refers to forgeries that exchange one person’s facial features with another, changing the original identity of the depicted person. Representative datasets of this type include CelebDF-v2 [46].
- **Face Swap (Multiple Faces):** In our benchmark, this refers to forgeries that exchange more than one person’s facial features with other human faces in one media. Representative datasets of this type include OpenForensics [42].
- **Face Transfer:** In our benchmark, this refers to forgeries that transfer both the identity-aware and identity-agnostic content (such as the pose and expression) of the source face to the target face. This follows the design proposed in ForgeryNet [32].
- **Face Reenactment:** In our benchmark, this refers to forgeries that transfer the facial expressions, movements, and emotions of one person’s face to another person’s face. Representative datasets of this type include FF++ [75].
- **Copy-Move:** In our benchmark, this refers to forgeries that involve copying a portion of an image and pasting it elsewhere within the same image. Representative datasets of this type include HiFi-IFDL [30].
- **Removal:** In our benchmark, this refers to forgeries that involve removing an object or region from an image and filling in the removed area to maintain the visual coherence, which is also known as “inpainting”. Representative datasets of this type include HiFi-IFDL [30].

Forgery Task	Forgery Semantic	Forgery Type	Forgery Model	Forgery Modality	Data Sources	Sample Number
Forgery Spatial Localization (Segmentation)	Human Subject	Face Reenactment	Graphics-based methods	RGB Images	FF++(Face2Face) [75]; ForgeryNet(FirstOrderMotion) [32]	200
Forgery Spatial Localization (Segmentation)	Human Subject	Face Reenactment	Encoder-Decoder	RGB Images	ForgeryNet(ATVG-Net) [32]; ForgeryNet(Talking-head Video) [32]	200
Forgery Spatial Localization (Segmentation)	Human Subject	Face Reenactment	Recurrent Neural Networks	RGB Images	HiFi-IFDL(STGAN) on CelebAHQ) [30]; DFFD(StarGAN2+BlendFace) [32]; ForgeryNet(StarGAN-2) [32]; ForgeryNet(MaskGAN) [32]; ForgeryNet(SC-PEGAN) [32]	400
Forgery Spatial Localization (Segmentation)	Human Subject	Face Editing	Encoder-Decoder	RGB Images	HiFi-IFDL(STGAN) on CelebAHQ) [30]; DFFD(StarGAN2+BlendFace) [32]; ForgeryNet(StarGAN2) [32]	800
Forgery Spatial Localization (Segmentation)	Human Subject	Face Editing	Proprietary	RGB Images	DFFD(FaceAPP on FFHQ) [15]; ForgeryNet(StarGAN2+BlendFace) [32]; ForgeryNet(StyleGANv2) [32]; ForgeryNet(DiscoFaceGAN) [32]	200
Forgery Spatial Localization (Segmentation)	Human Subject	Face Editing	Encoder-Decoder;Graphics-based methods	RGB Images	ForgeryNet(StarGAN2+BlendFace) [32]	200
Forgery Spatial Localization (Segmentation)	Human Subject	Face Swap (Single Face);Face Editing	Encoder-Decoder	Videos	ForgeryNet(DeepFaceLab-StarGAN2) [32]	100
Forgery Spatial Localization (Segmentation)	Human Subject	Face Swap (Single Face);Face Editing	Encoder-Decoder	RGB Images	ForgeryNet(DeepFaceLab-StarGAN2) [32]	200
Forgery Spatial Localization (Segmentation)	General Subject	Copy&Move	Graphics-based methods	RGB Images	HiFi-IFDL(PSCC-Net) [30]	200
Forgery Spatial Localization (Segmentation)	General Subject	Removal	Encoder-Decoder	RGB Images	HiFi-IFDL(PSCC-Net) [30]	200
Forgery Spatial Localization (Segmentation)	General Subject	Splicing	Graphics-based methods	RGB Images	HiFi-IFDL(PSCC-Net) [30]	200
Forgery Spatial Localization (Segmentation)	Human Subject	Entire Synthesis	Generative Adversarial Networks	RGB Images	DFFD(ProGAN) [15]; DFFD(StyleGANv1) [15]; ForgeryNet(StyleGANv2) [32]; ForgeryNet(DiscoFaceGAN) [32]	800
Forgery Spatial Localization (Segmentation)	Human Subject	Face Swap (Multiple Faces)	Generative Adversarial Networks	RGB Images	OpenForensics [42]	200
Forgery Spatial Localization (Detection)	Human Subject	Face Swap (Multiple Faces)	Generative Adversarial Networks	RGB Images	OpenForensics [42]	200
Forgery Spatial Localization (Segmentation)	Human Subject	Face Swap (Multiple Faces)	Graphics-based methods,Recurrent Neural Networks,Encoder-Decoder	Videos	FFIW(DeepFaceLab, FSGAN, FaceSwap) [114]	200
Forgery Spatial Localization (Segmentation)	Human Subject	Face Swap (Multiple Faces)	Graphics-based methods,Recurrent Neural Networks,Encoder-Decoder	RGB Images	FFIW(DeepFaceLab, FSGAN, FaceSwap) [114]	200
Forgery Spatial Localization (Detection)	Human Subject	Face Swap (Single Face)	Encoder-Decoder	RGB Images,Texts	DGM4(SimSwap) [78]; DGM4(InfoSwap) [78]	400
Forgery Spatial Localization (Detection)	Human Subject	Face Editing	Encoder-Decoder	RGB Images,Texts	DGM4(HFGI) [78]	200
Forgery Spatial Localization (Detection)	Human Subject	Face Editing	Generative Adversarial Networks	RGB Images,Texts	DGM4(StyleCLIP) [78]	200
Forgery Spatial Localization (Detection)	Human Subject	Text Swap	Retrieval-based methods	RGB Images,Texts	DGM4(retrieval) [78]	200
Forgery Spatial Localization (Detection)	Human Subject	Text Attribute Manipulation	Transformer	RGB Images,Texts	DGM4(B-GST) [78]	200
Forgery Spatial Localization (Detection)	Human Subject	Face Swap (Single Face),Text Swap	Encoder-Decoder,Retrieval-based methods	RGB Images,Texts	DGM4(SimSwap+B-GST) [78]; DGM4(InfoSwap+B-GST) [78]	400
Forgery Spatial Localization (Detection)	Human Subject	Face Editing,Text Swap	Encoder-Decoder,Retrieval-based methods	RGB Images,Texts	DGM4(HFGI+retrieval) [78]	200
Forgery Spatial Localization (Detection)	Human Subject	Face Editing,Text Swap	Generative Adversarial Networks,Retrieval-based methods	RGB Images,Texts	DGM4(StyleCLIP+B+retrieval) [78]	200
Forgery Spatial Localization (Detection)	Human Subject	Face Swap (Single Face),Text Attribute Manipulation	Encoder-Decoder,Transformer	RGB Images,Texts	DGM4(SimSwap+B-GST) [78]; DGM4(InfoSwap+B-GST) [78]	400
Forgery Spatial Localization (Detection)	Human Subject	Face Editing,Text Attribute Manipulation	Encoder-Decoder,Transformer	RGB Images,Texts	DGM4(HFGI+B-GST) [78]	200
Forgery Spatial Localization (Detection)	Human Subject	Face Editing,Text Attribute Manipulation	Generative Adversarial Networks,Transformer	RGB Images,Texts	DGM4(StyleCLIP+B-GST) [78]	200
Forgery Temporal Localization	Human Subject	Face Swap (Single Face)	Encoder-Decoder	Videos	ForgeryNet(DeepFaceLab) [32]; ForgeryNet(FaceShifter) [32]	400
Forgery Temporal Localization	Human Subject	Face Swap (Single Face)	Recurrent Neural Networks	Videos	ForgeryNet(FSGAN) [32]	200
Forgery Temporal Localization	Human Subject	Face Transfer	Graphics-based methods	Videos	ForgeryNet(BlendFace) [32]; ForgeryNet(MMR Replacement) [32]	300
Forgery Temporal Localization	Human Subject	Face Reenactment	Recurrent Neural Networks	Videos	ForgeryNet(ATVG-Net) [32]; ForgeryNet(Talking-head Video) [32]	400
Forgery Temporal Localization	Human Subject	Face Swap (Single Face),Face Editing	Encoder-Decoder	Videos	ForgeryNet(DeepFaceLab-StarGAN2) [32]	200
Forgery Binary Classification	Human Subject	Real	Real	RGB Images,Texts	DGM4 [78]	2000
Forgery Binary Classification	Human Subject	Real	Real	RGB Images	DFFD(ProGAN) [15]; DiffusionForensics(CelebAHQ) [92]; DeeperForensics [36]; FF++ [73]; CelebDF-v2 [46]; FFIW [114]; Celeba-Spoof [109]	4000
Forgery Binary Classification	General Subject	Real	Real	RGB Images	FF++ [73]; CelebDF-v2 [46]; DeeperForensics [36]; FFIW [114]; Celeba-Spoof [109]	178
Forgery Spatial Localization (Segmentation)	Human Subject	Real	Real	RGB Images	DFFD(FFHQ) [15]; DiffusionForensics(CelebAHQ) [92]; DeeperForensics [36]; FF++ [73]; CelebDF-v2 [46]; FFIW [114]; Celeba-Spoof [109]	1600
Forgery Spatial Localization (Segmentation)	General Subject	Real	Real	RGB Images	CNN-spot [89]; DiffusionForensics(LSUN, ImageNet) [92]; COCO2017val [51]	1500
Forgery Spatial Localization (Segmentation)	Human Subject	Real	Real	Videos	FF++ [73]; CelebDF-v2 [46]; DeeperForensics [36]; FFIW [114]; Celeba-Spoof [109]	178
Forgery Spatial Localization (Detection)	Human Subject	Real	Real	RGB Images	DFFD(FFHQ) [15]; DiffusionForensics(CelebAHQ) [92]; DeeperForensics [36]; FF++ [73]; CelebDF-v2 [46]; FFIW [114]; Celeba-Spoof [109]	1000
Forgery Spatial Localization (Detection)	Human Subject	Real	Real	RGB Images	FF++ [73]; CelebDF-v2 [46]; DeeperForensics [36]; FF++ [73]; CelebDF-v2 [46]; FFIW [114]; Celeba-Spoof [109]	1100
Forgery Spatial Localization (Detection)	General Subject	Real	Real	RGB Images	CNN-spot [89]; DiffusionForensics(LSUN, ImageNet) [92]	1000
Forgery Temporal Localization	Human Subject	Real	Real	Videos	ForgeryNet [32]	378

Table 8. Forensics-Bench data structure (part 3): including the detailed information of 5 designed perspectives characterizing forgeries, sample number and data sources collected under licenses.

- **Splicing:** In our benchmark, this refers to forgeries that involve combining elements from two or more different images to create a composite image. Representative datasets of this type include HiFi-IFDL [30].
- **Image Enhancement:** In our benchmark, this refers to forgeries where enhancements are deliberately applied to alter the appearance of an image, such as image super-resolution and low-light imaging. Representative datasets of this type include CNN-spot [89].
- **Out-of-Context:** In our benchmark, this refers to forgeries where the presentation of an authentic image, video, or media clip is repurposed with a misleading or deceptive text. Representative datasets of this type include NewsCLIPpings [60].
- **Style Translation:** In our benchmark, this refers to forgeries which transform the visual style of one image while preserving the content of another image. Representative datasets of this type include CNN-spot [89].
- **Text Attribute Manipulation:** In our benchmark, this refers to forgeries that alter the sentiment tendency of a given text while preserving its core content or meaning. This follows the design in DGM4 [78].

Keys	Example 1	Example 2
Image Path	/path/to/image	/path/to/image
Image Resolution	299x299	1280x720
Data Source	DFFD.StyleGANv1_ffhq	ForgeryNet.12_seg
Forgery Semantic	Human	Human
Forgery Modality	RGB Image	RGB Image
Forgery Task	Forgery Binary Classification	Forgery Spatial Localization (Segmentation)
Forgery Type	Entire Synthesis	Face Editing
Forgery Model	Generative Adversarial Networks	Encoder-Decoder
Question Template	What is the authenticity of the image? [AI-generated, non AI-generated]	Which segmentation map denotes the forged area in the image most accurately? [Candidate 1, Candidate 2, Candidate 3, Candidate 4]
Choice List		Candidate 4
Answer		

Table 9. Examples of the uniformed metadata.

- **Text Swap:** In our benchmark, this refers to forgeries that alter the overall semantic of a text with word substitution while preserving words regarding the main character. This follows the design in DGM4 [78].
- **Face Editing & Text Attribute Manipulation:** In our benchmark, this refers to forgeries that are produced under the combination of both Face Editing & Text Attribute Manipulation. This follows the design in DGM4 [78].
- **Face Editing & Text Swap:** In our benchmark, this refers to forgeries that are produced under the combination of both Face Editing & Text Swap. This follows the design in DGM4 [78].
- **Face Editing & Face Transfer:** In our benchmark, this refers to forgeries that are produced under the combination of both Face Editing & Face Transfer. This follows the design in ForgeryNet [32].
- **Face Swap (Single Face) & Face Editing:** In our benchmark, this refers to forgeries that are produced under the combination of both Face Swap (Single Face) & Face Editing. This follows the design in ForgeryNet [32].
- **Face Swap (Single Face) & Text Attribute Manipulation:** In our benchmark, this refers to forgeries that are produced under the combination of both Face Swap (Single Face) & Text Attribute Manipulation. This follows the design in DGM4 [78].
- **Face Swap (Single Face) & Text Swap:** In our benchmark, this refers to forgeries that are produced under the combination of both Face Swap (Single Face) & Text Swap. This follows the design in DGM4 [78].

Details of forgery models. In our benchmark, we roughly divide previous forgeries into 22 categories from the perspective of forgery model. We summarize the details as follows.

- **Generative Adversarial Networks:** In our benchmark, this refers to forgeries that are generated with vanilla GANs, namely a pair of adversarially trained generator and discriminator. Representative datasets of this category include CNN-spot [89].
- **Diffusion models:** In our benchmark, this refers to forgeries that are generated with vanilla diffusion models, such as DDPM [33]. Representative datasets of this category include DiffusionForensics [92].
- **Encoder-Decoder:** In our benchmark, this represents forgery models which commonly take real media as input, and are typically used to separate the identity information from identity-agnostic attributes, then alter or exchange the facial representations. This kind of models usually features an encoder-decoder structure. This follows the design in ForgeryNet [32] and representative datasets of this category include CelebDF-v2 [46] and FF++ [75].
- **Recurrent Neural Networks:** In our benchmark, this represents forgery models which are commonly used to alter sequential and dynamic-length data like videos. This follows the design in ForgeryNet [32].
- **Proprietary:** In our benchmark, this represents closed-source forgery models commonly used for commercial purposes, like Midjourney. Representative datasets of this category include GenImage [116].
- **3D masks:** In our benchmark, this represents forgeries which are produced based on 3D masks designed to look like real users, commonly used for face spoofing. Representative datasets of this category include CelebA-Spoof [109].
- **Print:** In our benchmark, this represents forgeries which are produced based on a printed photograph of a face, in order to trick facial recognition systems. Representative datasets of this category include CelebA-Spoof [109].
- **Paper-Cut:** In our benchmark, this represents forgeries which are produced based on a printed photograph of a face with specific modifications, such as eye and mouth cutouts. Representative datasets of this kind include CelebA-Spoof [109].
- **Replay:** In our benchmark, this represents forgeries which are produced by displaying a recorded video or image sequence of the face on a screen. Representative datasets of this category include CelebA-Spoof [109].
- **Transformer:** In our benchmark, this represents forgery models that are mainly used to modify texts, such as altering the sentiment tendency. Representative datasets of this category include DGM4 [78].
- **Decoder:** In our benchmark, this represents forgery models which are mainly used to perform style translations, commonly featuring a decode-only structure. Representative datasets of this category include CNN-spot [89].
- **Graphics-based methods:** In our benchmark, this represents forgeries that are mainly produced with traditional graphics

formations. This follows the design in ForgeryNet [32].

- Retrieval-based methods: In our benchmark, this represents forgeries that are produced by retrieving existing data. Representative datasets of this category include DGM4 [78].
- Unknown (in the wild): In our benchmark, this represents forgeries with unknown sources. Representative datasets of this category include DFPCP [17].
- Variational Auto-Encoders: In our benchmark, this represents forgeries that are generated with typical Variational Auto-Encoders. Representative datasets of this category include DeeperForensics [36].
- Auto-regressive models: In our benchmark, this represents forgery models which are commonly used to generate video data with no basis of real media, such as CogVideo [34].
- Encoder-Decoder&Retrieval-based methods: In our benchmark, this represents forgeries that are produced under the combination of Encoder-Decoder&Retrieval-based methods. This follows the design in DGM4 [78].
- Encoder-Decoder&Recurrent Neural Networks&Graphics-based methods: In our benchmark, this represents forgeries that are produced under the combination of Encoder-Decoder&Recurrent Neural Networks&Graphics-based methods. Representative datasets of this category include FFIW [114].
- Generative Adversarial Networks&Retrieval-based methods: In our benchmark, this represents forgeries that are produced by the combination of Generative Adversarial Networks&Retrieval-based methods. This follows the design in DGM4 [78].
- Encoder-Decoder&Transformer: In our benchmark, this represents forgeries that are produced under the combination of Encoder-Decoder&Transformer. This follows the design in DGM4 [78].
- Generative Adversarial Networks&Transformer: In our benchmark, this represents forgeries that are produced under the combination of Generative Adversarial Networks&Transformer. This follows the design in DGM4 [78].
- Encoder-Decoder&Graphics-based methods: In our benchmark, this represents forgeries that are produced under the combination of Encoder-Decoder&Graphics-based methods. This follows the design in ForgeryNet [32].

Details of forgery tasks. In our benchmark, we roughly divide previous forgeries into 4 categories from the perspective of forgery task. We summarize the details as follows.

- Forgery Binary Classification: This task aims to identify whether a given input (image, video, or text) is genuine or fake (forged). For instance, we can design the question template as *What is the authenticity of the image?* with two choice selections *AI-generated* and *non AI-generated* for HS-RGB-BC-ES-GAN (Please refer to Table 5 for the full term).
- Forgery Spatial Localization (Detection): This task aims to determine the specific regions within the input that have been altered, tampered with, or manipulated. For instance, we can design the question template as *Please detect the forged area in this image and the forged text in the corresponding caption:* “*Gen Prayuth Chanocha says democracy will only return after reforms are put in place*”. *The output format for the forged area should be a list of bounding boxes, namely [x, y, w, h], representing the coordinates of the top-left corner of the bounding box, as well as the width and height of the bounding box. The width of the input image is 624 and the height is 351. The output format for the forged text should be the a list of token positions in the whole caption, where the initial position index starts from 0. The token length of the input caption is 14..* The corresponding choice list is: A. { “forged area”: [[274, 46, 358, 167]], “forged text”: [] }, B. { “forged area”: [[274, 46, 358, 167], [220, 35, 330, 169]], “forged text”: [5] }, C. { “forged area”: [[274, 46, 358, 167], [186, 122, 333, 196]], “forged text”: [1, 6] }, D. { “forged area”: [[274, 46, 332, 141], [1, 120, 295, 192]], “forged text”: [] }. This example is for HS-RGB&TXT-SLD-FE-ED (Please refer to Table 5 for the full term).
- Forgery Spatial Localization (Segmentation): This task aims to precisely outline the regions of tampered or manipulated content within the digital media using pixel-wise classification. For instance, we can design the question template as *Which segmentation map denotes the forged area in the image most accurately?* with four choice selections [Candidate 1, Candidate 2, Candidate 3, Candidate 4], each of which points to a segmentation map. This example is for HS-RGB-SLS-FE-ED (Please refer to Table 5 for the full term).
- Forgery Temporal Localization: This task aims to detect the tampered or manipulated segments within a video. For instance, we can design the question template as *Please locate the forged frames in the given set of frames, which are sampled from a video.* *The output format should be the a list of indexes indicating the forged frames. The initial index starts from 0..* The corresponding choice list is: A. [0, 1, 5], B. [1], C. [0], D. [0, 1]. This example is for HS-VID-TL-FSS-ED (Please refer to Table 5 for the full term).

9. LVLMs Model Details

In this section, we present the summary of the LVLMs utilized in this paper, detailing their parameter sizes, visual encoders, and LLMs, which is shown in Table 10. We follow the evaluation tool [22] provided in OpenCompass [12] for the evaluations.

Models	Parameters	Vision Encoder	LLM
GPT4o [69]	-	-	-
Gemini1.5 ProVision [84]	-	-	-
Claude3.5-Sonnet [1]	-	-	-
LLaVA-Next-34B [54]	34.8B	CLIP ViT-L/14	Nous-Hermes-2-Yi-34B
LLaVA-v1.5-7B-XTuner [13]	7.2B	CLIP ViT-L/14	Vicuna-v1.5-7B
LLaVA-v1.5-13B-XTuner [13]	13.4B	CLIP ViT-L/14	Vicuna-v1.5-13B
InternVL-Chat-V1-2 [8, 86]	40B	InternViT-6B	Nous-Hermes-2-Yi-34B
LLaVA-NEXT-13B [54]	13.4B	CLIP ViT-L/14	Vicuna-v1.5-13B
mPLUG-Owl12 [101]	8.2B	CLIP ViT-L/14	LLaMA2-7B
LLaVA-v1.5-7B [52, 53]	7.2B	CLIP ViT-L/14	Vicuna-v1.5-7B
LLaVA-v1.5-13B [52, 53]	13.4B	CLIP ViT-L/14	Vicuna-v1.5-13B
Yi-VL-34B [103]	34.6B	CLIP ViT-H/14	Nous-Hermes-2-Yi-34B
CogVLM-Chat [90]	17B	EVA-CLIP-E	Vicuna-v1.5-7B
XComposer2 [21]	7B	CLIP ViT-L/14	InternLM2-7B
LLaVA-InternLM2-7B [13]	8.1B	CLIP ViT-L/14	InternLM2-7B
VisualGLM-6B	8B	EVA-CLIP	ChatGLM-6B
LLaVA-NEXT-7B [54]	7.1B	CLIP ViT-L/14	Vicuna-v1.5-7B
LLaVA-InternLM-7B [13]	7.6B	CLIP ViT-L/14	InternLM-7B
ShareGPT4V-7B [7]	7.2B	CLIP ViT-L/14	Vicuna-v1.5-7B
InternVL-Chat-V1-5 [8, 86]	40B	InternViT-6B	Nous-Hermes-2-Yi-34B
DeepSeek-VL-7B [58]	7.3B	SAM-B & SigLIP-L	DeekSeek-7B
Yi-VL-6B [103]	6.6B	CLIP ViT-H/14	Yi-6B
InstructBLIP-13B [14]	13B	EVA-CLIP ViT-G/14	Vicuna-v1.5-13B
Qwen-VL-Chat [2]	9.6B	CLIP ViT-G/16	Qwen-7B
Monkey-Chat [48]	9.8B	CLIP-ViT-BigHuge	Qwen-7B

Table 10. Model architecture of 25 LVLMs evaluated on Forensics-Bench.

10. Additional Experiments

Single-image input vs Multi-images input. The ability to process multiple images is essential for large vision language models, which may also facilitate LVLMs to understand forgeries of sequential data like videos. For example, frames of a real video may transition smoothly and naturally, whereas a fake video may exhibit inter-frame inconsistencies. To this end, we propose to analyze the effects of single-image prompt and multi-images prompt on LVLMs with capabilities to understand multiple images. Specifically, we collect the subset of our Forensics-Bench featuring video modality, and feed LVLMs with single-image input and multi-images input. Note that the single-image input is generated by piecing together sampled frames into one big input image, as shown in Figure 1. The results are demonstrated in Table 11, where the evaluated LVLMs also support multiple images as input. We find that LVLMs, like InternVL-Chat-V1-2 and Gemini-1.5-Pro, effectively exploited the relations among frames to perform forgery detections, while other LVLMs faced challenges in extracting meaningful information to determine the authenticity of the input frames, highlighting the unique difficulties of video forgery detections.

Experiments on prompt engineering. In the main paper, we mainly focused on baseline evaluations, following the Open-Compass [12] protocol and using default system prompts recommended by each LVLM, which are already well-trained. Nevertheless, beyond the baseline results, we have conducted experiments, adding a new forgery-related prompt: “*Please make your decision using forgery detection techniques, such as examining facial features, blending artifacts, lighting irregularities, and any other inconsistencies that may indicate manipulations.*”. Results in Table 12 show guiding LVLMs to focus on such forgery traces boosted performance to some extent, which may inspire future studies.

More experiments on forgery attribution. In this section, we explore methods to enhance LVLMs’ performance on the task of forgery attribution. To this end, we have conducted experiments by adding detailed introductions of different forgery models into the prompt, as detailed in Appendix 8, aiming to reduce LVLMs’ potential misunderstandings for forgery attribution. Results in Table 13 show that this improved LVLMs’ performance, which may inspire future studies.

Experiments on visual prompt engineering. In this section, we have conducted experiments where we added bounding

Model	InternVL-Chat-V1-2	mPLUG-Owl2	Gemini-1.5-Pro	InternVL-Chat-V1-5	Qwen-VL-Chat	Claude3V-Sonnet
Single-Image Prompt	62.9	59.8	38.8	52.2	38.9	35.9
Multi-Images Prompt	63.9	36.3	40.9	34.8	25.7	30.2

Table 11. The performance comparison between single-image input and multi-images input.

Model	Baseline	+Prompt Engineering
LLaVA-v1.5-7B-XTuner	65.7	67.6
LLaVA-v1.5-13B-XTuner	65.2	67.1
LLaVA-NEXT-13B	58.0	61.3

Table 12. Experiments on prompt engineering.

Model	Baseline	+Detailed Introductions of Forgery Models
LLaVA-NEXT-34B	44.0	55.7
InternVL-Chat-V1-2	41.6	55.6
LLaVA-v1.5-7B-XTuner	42.2	49.6
mPLUG-Owl2	39.9	45.4

Table 13. More experiments on forgery attribution.

Model	Baseline	+Prompt Engineering (Visual)
LLaVA-v1.5-7B-XTuner	83.5	87.6
LLaVA-NEXT-34B	84.1	85.7
InternVL-Chat-V1-2	84.5	86.5
LLaVA-NEXT-13B	68.2	70.4

Table 14. Experiments on visual prompt engineering.

Model	HS-RGB-BC-ES-DF	HS-NIR-BC-ES-GAN	HS-RGB-BC-ES-GAN	HS-RGB-SLS-ES-GAN	HS-RGB-BC-ES-PRO	HS-RGB-BC-SPF-3D	HS-RGB-BC-SPF-PC	HS-RGB-BC-SPF-PR	HS-RGB-BC-SPF-RP	HS-RGB-BC-FE-DF
LLaVA-NEXT-34B	90.8%	100.0%	85.4%	19.3%	97.0%	100.0%	99.0%	90.0%	72.0%	95.2%
LLaVA-v1.5-7B-XTuner	79.8%	100.0%	68.9%	25.0%	87.0%	99.5%	99.0%	67.0%	37.5%	99.0%
LLaVA-v1.5-13B-XTuner	85.9%	99.9%	70.4%	23.6%	92.5%	100.0%	100.0%	97.5%	86.5%	100.0%
InternVL-Chat-V1-2	67.6%	87.3%	57.9%	18.8%	78.0%	98.0%	99.5%	86.5%	55.0%	94.8%
LLaVA-NEXT-13B	88.9%	100.0%	80.3%	24.3%	93.5%	100.0%	100.0%	99.5%	96.0%	85.3%
GPT4o	86.2%	96.6%	72.7%	22.1%	92.5%	94.0%	91.0%	45.5%	24.5%	95.0%
mPLUG-Owl2	88.7%	99.9%	62.7%	28.8%	94.5%	100.0%	99.5%	98.5%	91.0%	99.7%
LLaVA-v1.5-7B	49.2%	100.0%	48.7%	36.0%	58.5%	100.0%	100.0%	97.5%	87.5%	95.3%
LLaVA-v1.5-13B	53.5%	99.0%	42.9%	37.6%	63.0%	100.0%	100.0%	91.5%	59.0%	78.2%
Yi-VL-34B	59.3%	77.1%	24.6%	23.8%	82.5%	84.5%	56.5%	35.5%	19.5%	65.3%
CogVLM-Chat	47.4%	52.8%	51.8%	25.9%	45.0%	83.5%	78.5%	40.0%	38.0%	61.8%
Gemini-1.5-Pro	54.0%	33.3%	45.0%	14.8%	59.0%	26.0%	76.5%	17.5%	12.5%	69.3%
XComposers2	44.2%	50.8%	31.7%	10.0%	55.0%	94.0%	90.0%	38.5%	35.0%	34.3%
LLaVA-InternLM-2B-7B	22.4%	73.2%	20.7%	31.5%	28.5%	95.0%	99.5%	73.5%	31.5%	41.2%
VisualGIM-6B	32.9%	49.1%	56.9%	24.1%	49.0%	55.5%	57.0%	27.5%	21.5%	53.8%
LLaVA-InternLM-7B	42.2%	58.3%	40.3%	24.5%	67.5%	100.0%	100.0%	97.0%	91.5%	36.0%
ShareGPT4V-7B	13.9%	57.3%	17.3%	47.9%	24.0%	99.0%	100.0%	87.0%	55.5%	27.2%
InternVL-Chat-V1-5	15.9%	0.5%	14.1%	4.3%	22.0%	96.5%	97.0%	32.5%	24.0%	29.7%
DeepSeek-7B	29.4%	16.0%	17.2%	24.4%	45.0%	97.5%	99.0%	48.5%	34.5%	45.0%
Yi-VL-6B	32.4%	2.5%	6.3%	23.0%	60.5%	83.0%	70.5%	40.5%	45.0%	70.0%
InstructBLIP-13B	22.5%	73.3%	17.2%	25.0%	30.5%	58.5%	57.5%	42.5%	41.0%	33.7%
Qwen-VL-Chat	26.7%	36.1%	13.5%	23.5%	43.0%	50.5%	54.5%	23.5%	28.5%	28.7%
Claude3V-Sonnet	47.9%	19.8%	6.0%	13.3%	59.5%	55.0%	37.0%	4.0%	2.0%	51.5%
Monkey-Chat	12.2%	15.3%	7.6%	23.6%	27.0%	49.5%	50.0%	19.5%	19.0%	23.3%

Table 15. Detail results of 25 LVLMs on 112 forgery detection types (part 1).

boxes to human subjects for forgery binary classification and prompted LVLMs to focus on these image regions. Table 14 shows that such visual prompts boosted performance to some extent, which may inspire future studies.

11. Detailed Performance of LVLMs on Forensics-Bench

From Table 15 to Table 26, we present the detailed performance of 25 state-of-the-art LVLMs across 112 forgery detection types, with the accuracy as the metric. Please refer to Table 5 for the full term of each column title.

Model	HS-RGB-BC-FE-ED	HS-RGB-SLS-FE-ED	HS-RGB&TXT-BC-FE-ED	HS-RGB&TXT-SLD-FE-ED	HS-RGB&TXT-BC-FE-GAN	HS-RGB&TXT-SLD-FE-GAN	HS-RGB-BC-FE-PRO	HS-RGB-SLS-FE-PRO	HS-RGB-BC-FE&FT-ED&GR	HS-RGB-SLS-FE&FT-ED&GR
LLaVA-NEXT-34B	99.1%	23.3%	73.0%	19.5%	79.0%	18.5%	92.5%	28.5%	100.0%	23.3%
LLaVA-v1.5-7B-XTuner	97.8%	23.6%	70.0%	15.5%	72.0%	15.5%	95.0%	21.0%	96.5%	23.3%
LLaVA-v1.5-13B-XTuner	100.0%	24.5%	89.0%	0.5%	93.5%	2.0%	99.5%	22.5%	100.0%	20.5%
InternVL-Chat-V1.2	96.5%	14.5%	54.5%	36.0%	59.5%	33.5%	85.0%	30.5%	97.0%	6.5%
LLaVA-Internal-T-13B	99.1%	20.4%	84.5%	1.0%	91.5%	1.5%	88.5%	27.0%	100.0%	26.0%
GPT4o	87.6%	24.0%	11.5%	5.5%	15.5%	2.5%	60.0%	24.5%	63.5%	17.7%
mpPLUG-Owl2	92.7%	24.4%	72.5%	29.5%	75.5%	25.5%	95.5%	31.0%	86.5%	21.5%
LLaVA-v1.5-7B	98.7%	25.5%	95.5%	10.5%	95.5%	7.0%	88.5%	21.5%	98.5%	24.0%
LLaVA-v1.5-13B	92.1%	23.0%	59.0%	2.0%	66.0%	3.0%	61.5%	27.0%	93.5%	27.0%
Vi-VL-34B	70.8%	24.5%	13.5%	26.5%	14.0%	21.5%	39.5%	27.5%	90.5%	24.5%
CogVLM-Chat	74.4%	23.8%	75.0%	18.5%	74.5%	24.5%	56.5%	28.0%	57.0%	23.5%
Qwen-Chat	79.5%	29.0%	27.5%	32.5%	24.5%	3.5%	99.5%	33.0%	60.5%	23.5%
XCompson2	66.4%	12.3%	23.5%	26.5%	31.0%	26.0%	22.5%	20.0%	74.0%	11.0%
LLaVA-Internal-M-7B	62.8%	22.0%	19.0%	13.5%	28.5%	10.0%	16.5%	27.0%	68.5%	23.5%
VisualGLM-6B	53.3%	24.4%	21.0%	17.0%	19.0%	25.0%	91.0%	24.0%	66.5%	22.5%
LLaVA-NEXT-1B	66.3%	23.1%	94.5%	6.0%	94.5%	5.5%	14.5%	25.0%	88.0%	20.0%
LLaVA-Internal-M-7B	61.1%	27.4%	28.0%	43.0%	25.5%	29.5%	29.5%	27.5%	60.5%	22.5%
StableDiffusion	58.1%	23.9%	96.5%	15.5%	96.5%	13.0%	10.5%	25.5%	70.0%	24.0%
InternVL-Chat-V1.5	57.9%	5.0%	26.5%	31.0%	27.5%	33.0%	19.0%	28.5%	74.5%	1.5%
DeepSeek-VL-7B	62.6%	19.1%	8.0%	29.5%	9.0%	32.0%	20.5%	26.5%	64.5%	15.5%
Vi-VL-6B	68.2%	24.6%	21.5%	25.5%	27.0%	21.0%	51.5%	28.5%	60.0%	29.5%
InstructBLIP-13B	55.1%	25.5%	2.5%	14.0%	3.0%	21.5%	29.5%	21.5%	45.5%	25.0%
Qwen-VL-Chat	34.1%	25.0%	28.5%	22.0%	38.5%	20.0%	11.5%	27.5%	36.0%	25.5%
Claude3-V-Sonnet	35.7%	23.5%	21.0%	16.0%	18.0%	17.5%	22.0%	29.0%	30.5%	21.0%
Monkey-Chat	26.9%	23.5%	6.5%	26.5%	11.0%	30.0%	13.0%	30.5%	30.0%	22.5%

Table 16. Detail results of 25 LVLMs on 112 forgery detection types (part 2).

Model	HS-RGB&TXT-BC-FE&TAM-ED&TR	HS-RGB&TXT-SLD-FE&TAM-ED&TR	HS-RGB&TXT-BC-FE&TAM-GAN&TR	HS-RGB&TXT-SLD-FE&TAM-GAN&TR	HS-RGB&TXT-BC-FE&TS-ED&TR	HS-RGB&TXT-SLD-FE&TS-ED&TR	HS-RGB&TXT-BC-FE&TS-GAN&TR	HS-RGB&TXT-SLD-FE&TS-GAN&TR	
LLaVA-NEXT-34B	98.0%	20.5%	17.0%	87.5%	18.0%	87.5%	40.0%	99.5%	42.0%
LLaVA-v1.5-7B-XTuner	91.5%	22.0%	100.0%	100.0%	100.0%	100.0%	33.0%	90.0%	25.5%
LLaVA-v1.5-13B-XTuner	95.5%	10.0%	100.0%	100.0%	100.0%	100.0%	33.0%	92.5%	23.0%
InternVL-Chat-V1.2	90.0%	22.0%	95.0%	18.0%	92.5%	47.0%	96.0%	52.0%	15.0%
LLaVA-NEXT-1B	99.5%	4.5%	98.0%	4.0%	98.0%	19.0%	100.0%	100.0%	1.5%
GPT4o	40.0%	18.0%	100.0%	100.0%	100.0%	100.0%	10.0%	100.0%	1.5%
mpPLUG-Owl2	34.0%	12.4%	95.5%	23.0%	95.5%	55.0%	95.5%	66.0%	1.5%
LLaVA-v1.5-7B	99.5%	16.0%	100.0%	16.5%	100.0%	100.0%	24.5%	100.0%	25.0%
LLaVA-v1.5-13B	89.0%	9.0%	88.5%	10.5%	92.5%	30.0%	94.0%	23.0%	1.5%
Vi-VL-34B	63.0%	33.4%	98.5%	33.5%	98.5%	42.5%	94.0%	43.5%	1.5%
CogVLM-Chat	94.0%	26.5%	95.0%	24.5%	94.5%	32.0%	95.5%	28.5%	1.5%
Gemini-1.5-Pro	64.5%	34.0%	66.0%	31.5%	82.5%	27.0%	85.0%	22.0%	1.5%
XCompson2	56.0%	48.0%	61.0%	52.0%	74.0%	48.5%	75.0%	51.0%	1.5%
LLaVA-Internal-M-7B	98.0%	3.0%	98.0%	3.0%	98.0%	52.5%	98.0%	53.5%	1.5%
VisualGLM-6B	29.0%	25.0%	28.0%	24.0%	27.0%	31.0%	27.5%	27.5%	1.5%
LLaVA-NEXT-1B	100.0%	18.5%	100.0%	18.0%	98.5%	44.0%	100.0%	100.0%	43.0%
LLaVA-v1.5-7B	98.5%	18.0%	100.0%	18.0%	98.0%	38.0%	98.5%	38.5%	1.5%
ShareDP-TV-1B	99.5%	26.0%	100.0%	26.0%	99.5%	37.5%	98.5%	46.0%	1.5%
InternVL-Chat-V1.5	67.5%	17.5%	62.5%	22.0%	80.0%	27.0%	81.0%	27.0%	10.0%
DeepSeek-VL-7B	17.5%	13.5%	17.5%	17.0%	13.0%	20.0%	30.0%	17.0%	1.5%
Vi-VL-34B	3.5%	3.5%	3.5%	3.0%	3.5%	3.0%	3.5%	3.5%	1.5%
InstructBLIP-13B	3.5%	2.5%	2.5%	2.0%	3.0%	1.0%	3.5%	4.5%	2.5%
Qwen-VL-Chat	55.5%	21.0%	55.0%	21.5%	55.0%	32.5%	58.0%	25.5%	1.5%
Claude3-V-Sonnet	49.0%	15.5%	51.5%	10.0%	59.5%	15.0%	65.0%	15.0%	1.5%
Monkey-Chat	20.5%	21.0%	18.5%	22.0%	13.0%	27.0%	17.0%	23.0%	1.5%

Table 17. Detail results of 25 LVLMs on 112 forgery detection types (part 3).

Model	HS-VID-BC-FR-RNN	HS-VID-TL-FR-RNN	HS-RGB-BC-FR-RNN	HS-RGB-SLS-FR-RNN	HS-VID-BC-FR-ED	HS-RGB-BC-FR-ED	HS-RGB-SLS-FR-ED	HS-VID-BC-FR-GR	HS-VID-SLS-FR-GR	HS-RGB-BC-FR-GR
LLaVA-NEXT-34B	100.0%	14.8%	99.3%	26.3%	100.0%	90.0%	21.0%	100.0%	25.0%	77.0%
LLaVA-v1.5-7B-XTuner	99.8%	22.3%	94.3%	21.3%	99.3%	85.0%	28.5%	100.0%	20.0%	75.5%
LLaVA-v1.5-13B-XTuner	100.0%	25.5%	100.0%	23.8%	100.0%	100.0%	34.0%	100.0%	21.4%	100.0%
InternVL-Chat-V1.2	99.8%	23.3%	95.0%	11.5%	100.0%	90.0%	10.0%	100.0%	17.1%	85.0%
LLaVA-NEXT-1B	100.0%	14.0%	99.5%	23.3%	100.0%	91.3%	22.5%	100.0%	14.3%	88.5%
GPT4o	81.3%	22.5%	66.5%	28.8%	66.4%	39.0%	27.5%	70.0%	25.0%	7.0%
mpPLUG-Owl2	99.8%	27.8%	82.0%	24.5%	100.0%	72.8%	28.0%	100.0%	27.1%	67.5%
LLaVA-v1.5-7B	99.8%	18.0%	96.8%	20.8%	100.0%	89.0%	29.0%	100.0%	23.6%	84.5%
LLaVA-v1.5-13B	98.8%	23.0%	92.8%	24.8%	100.0%	74.0%	29.5%	99.3%	20.7%	66.5%
Vi-VL-34B	92.8%	26.3%	84.8%	27.8%	94.3%	83.5%	19.0%	95.7%	27.1%	81.5%
CogVLM-Chat	58.0%	21.8%	56.5%	27.3%	77.1%	56.0%	18.0%	69.3%	21.4%	51.5%
Gemini-1.5-Pro	48.3%	49.8%	54.3%	29.3%	71.1%	37.5%	33.0%	18.6%	44.3%	8.5%
XCompson2	68.3%	4.3%	73.0%	12.0%	19.3%	39.8%	13.0%	22.9%	49.3%	6.5%
LLaVA-Internal-M-7B	96.8%	17.5%	70.3%	21.0%	99.3%	45.3%	28.5%	98.6%	21.4%	17.0%
VisualGLM-6B	55.8%	33.0%	73.0%	26.0%	51.4%	69.0%	22.5%	60.7%	22.1%	78.0%
LLaVA-NEXT-7B	99.0%	23.8%	86.0%	22.5%	100.0%	54.3%	17.5%	99.3%	21.4%	41.5%
LLaVA-Internal-M-7B	48.0%	17.8%	65.0%	28.0%	38.6%	50.0%	25.0%	45.0%	21.4%	34.0%
ShareDP-TV-1B	84.5%	22.3%	66.8%	21.0%	86.4%	41.8%	28.0%	85.0%	21.4%	18.5%
InternVL-Chat-V1.5	96.3%	6.3%	70.8%	5.0%	91.4%	44.5%	5.5%	97.9%	5.0%	15.0%
DeepSeek-VL-7B	59.0%	8.5%	61.3%	19.5%	65.0%	37.5%	24.0%	62.9%	13.6%	7.0%
Vi-VL-6B	86.5%	25.3%	58.3%	28.0%	70.7%	40.3%	22.0%	64.3%	22.9%	25.0%
InstructBLIP-13B	85.0%	32.5%	45.3%	21.5%	88.6%	25.8%	28.0%	77.9%	30.7%	10.5%
Qwen-VL-Chat	55.0%	22.3%	37.0%	25.3%	47.1%	22.8%	22.5%	52.1%	23.6%	5.0%
Claude3-V-Sonnet	36.3%	14.1%	28.5%	18.5%	13.6%	15.3%	23.5%	15.0%	53.6%	2.5%
Monkey-Chat	9.8%	24.8%	30.0%	26.5%	9.3%	19.3%	19.0%	7.1%	22.1%	4.5%

Table 18. Detail results of 25 LVLMs on 112 forgery detection types (part 4).

Model	HS-RGB-SLS-FR-GF	HS-VID-BC-FSM-ED&RNN&GR	HS-VID-SLS-FSM-ED&RNN&GR	HS-RGB-BC-FSM-ED&RNN&GR	HS-RGB-SLS-FSM-ED&RNN&GR	HS-RGB-BC-FSM-GAN	HS-RGB-SLS-FSM-GAN	HS-VID-BC-FS-RNN	HS-VID-TL-FS-RNN	HS-RGB-BC-FS-RNN
LLaVA-NEXT-34B	20.0%	100.0%	26.0%	89.5%	23.0%	45.5%	20.0%	100.0%	4.5%	98.0%
LLaVA-v1.5-7B-XTuner	25.0%	100.0%	21.5%	77.0%	28.0%	15.5%	21.0%	100.0%	47.5%	93.0%
LLaVA-v1.5-7B-XTuner	21.5%	100.0%	26.5%	100.0%	27.0%	17.0%	20.0%	100.0%	3.8%	100.0%
InternVL-Chat-V1.2	95.5%	100.0%	23.5%	78.5%	24.5%	17.0%	100.0%	23.5%	93.0%	1.5%
LLaVA-NEXT-1B	21.5%	100.0%	18.0%	93.0%	19.5%	24.0%	20.5%	100.0%	18.5%	99.0%
GPT4o	21.5%	65.5%	15.0%	7.0%	21.0%	73.5%	19.5%	86.5%	19.5%	55.0%
mpPLUG-Owl2	25.0%	100.0%	28.5%	98.5%	25.5%	25.0%	21.0%	100.0%	43.5%	74.5%
LLaVA-v1.5-7B	25.5%	9.5%	28.5%	29.5%	25.5%	25.5%	23.5%	99.5%	4.5%	93.5%
VisualGLM-6B	51.5%	32.0%	38.5%	30.0%	43.5%	28.0%	58.0%	25.0%	68.0%	38.5%
LLaVA-NEXT-7B	19.5%	100.0%	29.5%	42.5%	17.0%	24.0%	99.5%	58.0%	80.0%	19.0%
LLaVA-Internal-M-7B	24.5%	48.0%	31.5%	20.5%	30.5%</td					

Model	HS-RGB-SLS-FSS-RNN	HS-RGB-BC-FSS-DF	HS-VID-BC-FSS-ED	HS-VID-SLS-FSS-ED	HS-VID-TL-FSS-ED	HS-RGB-BC-FSS-ED	HS-RGB-SLS-FSS-ED	HS-RGB&TXT-BC-FSS-ED	HS-RGB&TXT-SLD-FSS-ED	HS-VID-BC-FSS-GR
LLaVA-NEXT-34B	24.5%	95.5%	100.0%	18.4%	21.0%	75.4%	22.7%	78.5%	15.0%	100.0%
LLaVA-v1.5-7B-XTuner	27.5%	99.0%	99.9%	22.7%	12.8%	83.4%	25.4%	69.8%	16.5%	100.0%
LLaVA-v1.5-13B-XTuner	25.5%	100.0%	100.0%	22.3%	20.8%	100.0%	23.7%	93.8%	0.3%	100.0%
InternVL-Chat-V1-2	8.0%	96.3%	100.0%	20.1%	24.5%	84.2%	11.9%	57.8%	30.0%	100.0%
LLaVA-NEXT-13B	22.0%	94.8%	100.0%	13.9%	12.3%	83.6%	25.6%	89.8%	0.0%	100.0%
GPT4o	22.0%	96.0%	74.1%	22.7%	33.3%	34.9%	22.7%	16.5%	3.8%	74.3%
mPLUG-Owl2	25.0%	98.5%	99.9%	24.6%	18.3%	75.0%	22.9%	72.3%	35.5%	100.0%
LLaVA-v1.5-7B	28.0%	98.0%	100.0%	23.0%	17.0%	88.7%	25.6%	97.5%	10.3%	100.0%
LLaVA-v1.5-13B	28.0%	81.0%	99.9%	25.2%	14.5%	71.1%	25.4%	63.0%	2.0%	99.3%
Yi-VL-34B	24.5%	65.0%	97.7%	23.9%	22.3%	59.2%	22.9%	13.0%	26.8%	97.9%
CogVLM-Chat	24.5%	83.8%	62.4%	25.6%	20.8%	56.1%	23.1%	76.5%	19.3%	74.3%
Gemini-1.5-Pro	28.5%	87.5%	26.6%	18.4%	41.0%	24.9%	30.8%	31.5%	33.3%	23.6%
XCoposser2	12.5%	38.8%	39.1%	34.6%	6.5%	26.5%	10.0%	27.8%	25.5%	22.1%
LLaVA-NEXT-7B	20.4%	30.3%	98.6%	25.2%	20.5%	20.8%	25.6%	21.6%	11.0%	96.8%
VisualGLM-6B	23.5%	18.6%	53.6%	23.0%	33.3%	37.6%	20.4%	15.5%	20.0%	53.6%
LLaVA-NEXT-7B	25.0%	32.8%	95.6%	23.3%	9.5%	41.4%	18.9%	97.5%	6.5%	100.0%
LLaVA-InternLM-7B	30.5%	46.0%	49.7%	25.6%	13.3%	42.3%	28.3%	23.5%	45.5%	49.3%
ShareGPT4V-7B	27.5%	31.8%	87.5%	24.9%	9.5%	25.9%	26.1%	96.5%	15.5%	83.6%
InternVL-Chat-V1-5	6.0%	20.5%	92.0%	1.6%	11.3%	26.6%	4.7%	24.5%	28.8%	95.0%
DeepSeek-VL-7B	20.0%	33.3%	60.9%	8.4%	13.8%	22.8%	16.9%	5.8%	30.0%	62.9%
Yi-VL-6B	26.0%	74.0%	88.2%	23.3%	13.0%	28.1%	25.6%	24.3%	28.5%	75.0%
InstructBLIP-13B	26.5%	54.5%	86.3%	27.5%	26.5%	22.5%	24.1%	2.3%	20.8%	83.6%
Qwen-VL-Chat	21.0%	22.0%	56.7%	20.1%	20.5%	12.1%	23.6%	29.5%	26.8%	53.6%
Claude-IV-Sonnet	16.0%	38.5%	19.8%	41.7%	39.8%	8.1%	21.4%	19.5%	16.0%	20.0%
Monkey-Chat	24.0%	27.8%	6.8%	21.4%	17.0%	9.6%	21.6%	6.0%	30.0%	10.0%

Table 20. Detail results of 25 LVLMs on 112 forgery detection types (part 6).

Model	HS-VID-SLS-FSS-GR	HS-RGB-BC-FSS-GR	HS-RGB-SLS-FSS-GR	HS-VID-BC-FSS-WILD	HS-RGB-BC-FSS-WILD	HS-VID-BC-FSS-VAE	HS-RGB-BC-FSS-VAE	HS-VID-BC-FSS&FE-ED	HS-VID-SLS-FSS&FE-ED	HS-VID-TL-FSS&FE-ED
LLaVA-NEXT-34B	15.7%	74.0%	25.5%	100.0%	94.0%	100.0%	87.5%	100.0%	21.0%	15.0%
LLaVA-v1.5-7B-XTuner	27.1%	70.5%	23.0%	100.0%	78.0%	100.0%	77.5%	100.0%	22.0%	10.0%
LLaVA-v1.5-13B-XTuner	20.0%	99.5%	22.0%	100.0%	100.0%	100.0%	100.0%	100.0%	27.0%	23.5%
InternVL-Chat-V1-2	21.4%	88.5%	16.0%	100.0%	85.3%	100.0%	89.5%	100.0%	22.0%	25.5%
LLaVA-NEXT-13B	15.7%	90.5%	26.5%	100.0%	87.5%	100.0%	94.5%	100.0%	13.0%	11.5%
GPT4o	20.0%	24.5%	18.5%	48.8%	3.3%	76.0%	19.5%	84.5%	17.0%	28.5%
mPLUG-Owl2	20.7%	65.5%	23.5%	100.0%	47.0%	100.0%	75.5%	100.0%	27.0%	15.0%
LLaVA-v1.5-7B	20.2%	80.0%	21.5%	100.0%	95.8%	100.0%	86.5%	90.0%	22.0%	15.5%
LLaVA-v1.5-13B	17.9%	62.5%	25.5%	99.8%	77.6%	100.0%	68.0%	99.5%	26.0%	15.0%
Yi-VL-34B	20.0%	81.0%	25.6%	90.3%	32.2%	96.5%	77.0%	95.0%	28.0%	16.5%
CogVLM-Chat	20.0%	61.0%	25.5%	55.8%	49.5%	78.5%	53.5%	65.5%	26.0%	18.5%
Gemini-1.5-Pro	37.1%	19.5%	25.0%	18.5%	4.5%	40.5%	15.5%	56.0%	19.0%	41.0%
XCoposser2	35.7%	14.5%	13.0%	22.8%	2.8%	21.5%	8.5%	66.5%	50.0%	5.0%
LLaVA-InternLM-7B	20.0%	18.0%	23.5%	87.0%	2.0%	94.5%	19.0%	99.0%	26.0%	19.0%
VisualGLM-6B	28.6%	81.5%	25.5%	57.8%	58.3%	55.5%	68.0%	53.0%	24.0%	34.0%
LLaVA-NEXT-7B	16.4%	42.5%	19.5%	100.0%	31.8%	100.0%	40.5%	97.5%	24.0%	5.5%
LLaVA-InternLM-7B	20.0%	33.0%	30.0%	45.0%	24.0%	41.5%	47.5%	49.5%	26.0%	13.5%
ShareGPT4V-7B	20.0%	19.5%	19.0%	89.3%	41.8%	87.5%	23.0%	87.0%	26.0%	10.0%
InternVL-Chat-V1-5	3.6%	13.5%	4.0%	80.3%	1.8%	92.5%	10.0%	93.0%	1.0%	9.5%
DeepSeek-VL-7B	15.7%	8.5%	27.0%	57.0%	0.3%	63.5%	8.5%	67.0%	14.0%	1.0%
Yi-VL-34B	19.3%	25.5%	27.5%	97.5%	23.2%	70.0%	23.5%	89.5%	26.0%	12.0%
InstructBLIP-13B	25.7%	12.0%	23.5%	85.8%	24.0%	89.0%	16.0%	88.0%	23.0%	24.0%
Qwen-VL-Chat	23.6%	7.5%	25.5%	40.3%	4.3%	55.0%	4.5%	54.0%	22.0%	21.5%
Claude-IV-Sonnet	56.4%	3.0%	24.5%	2.0%	0.3%	13.0%	0.5%	46.0%	54.0%	43.5%
Monkey-Chat	15.0%	4.0%	26.0%	0.0%	0.5%	8.0%	3.0%	11.0%	24.0%	12.0%

Table 21. Detail results of 25 LVLMs on 112 forgery detection types (part 7).

Model	HS-RGB-BC-FSS&FE-ED	HS-RGB-SLS-FSS&FE-ED	HS-RGB&TXT-BC-FSS&TAM-ED&TR	HS-RGB&TXT-SLD-FSS&TAM-ED&TR	HS-RGB&TXT-BC-FSS&TS-ED&TR	HS-RGB&TXT-BC-FSS&TS-ED&RT	HS-RGB&TXT-SLD-FSS&TS-ED&RT	HS-RGB&TXT-BC-FT-GR	HS-VID-SLS-FT-GR	HS-VID-TL-FT-GR	HS-RGB-BC-FT-GR
LLaVA-NEXT-34B	100.0%	27.5%	99.0%	23.0%	84.5%	29.3%	44.3%	100.0%	16.9%	14.7%	94.5%
LLaVA-v1.5-7B-XTuner	98.5%	22.5%	93.0%	6.3%	98.0%	15.0%	100.0%	100.0%	19.9%	23.0%	100.0%
LLaVA-v1.5-13B-XTuner	100.0%	99.5%	100.0%	99.9%	99.8%	12.0%	100.0%	100.0%	13.4%	9.3%	99.8%
InternVL-Chat-V1-2	8.0%	99.5%	99.8%	7.5%	98.8%	12.0%	100.0%	100.0%	12.4%	12.4%	100.0%
LLaVA-NEXT-13B	100.0%	19.5%	99.8%	99.8%	99.8%	12.0%	100.0%	100.0%	13.4%	9.3%	99.8%
GPT4o	81.5%	21.0%	55.3%	43.0%	78.3%	33.3%	85.0%	100.0%	22.9%	12.7%	83.0%
mPLUG-Owl2	87.0%	25.0%	25.0%	27.0%	100.0%	10.0%	88.0%	100.0%	10.5%	16.0%	97.0%
LLaVA-v1.5-7B	94.5%	24.0%	99.0%	91.0%	92.5%	9.1%	94.0%	100.0%	12.4%	12.4%	97.0%
Yi-VL-34B	90.5%	24.5%	66.5%	34.8%	26.8%	41.3%	97.0%	23.8%	22.3%	88.3%	88.3%
CogVLM-Chat	69.0%	25.0%	97.3%	22.3%	96.3%	27.3%	66.3%	23.4%	18.0%	63.5%	63.5%
Gemini-1.5-Pro	34.3%	6.0%	60.0%	69.6%	38.3%	27.3%	62.7%	10.4%	47.0%	61.5%	61.5%
XCoposser2	8.5%	14.5%	14.5%	6.2%	9.5%	76.0%	84.9%	11.1%	11.1%	11.1%	73.5%
LLaVA-InternLM-7B	81.5%	21.0%	63.0%	34.3%	54.0%	57.3%	99.7%	23.8%	15.0%	73.5%	73.5%
VisualGLM-6B	78.5%	26.5%	26.3%	29.5%	21.3%	30.8%	55.3%	20.8%	34.3%	73.0%	73.0%
LLaVA-NEXT-7B	92.5%	18.0%	99.8%	24.3%	99.5%	42.5%	100.0%	15.2%	7.3%	86.0%	86.0%
LLaVA-v1.5-13B-XTuner	98.0%	10.0%	100.0%	100.0%	100.0%	10.0%	99.0%	100.0%	14.4%	14.4%	100.0%
ShareGPT4V-7B	71.0%	24.5%	100.0%	31.5%	100.0%	43.0%	92.0%	23.8%	11.7%	68.8%	68.8%
InternVL-Chat-V1-5	81.5%	4.0%	71.0%	19.8%	78.8%	31.3%	96.0%	0.9%	19.0%	73.8%	73.8%
DeepSeek-VL-7B	77.5%	20.0%	22.5%	21.8%	15.5%	20.0%	73.7%	4.3%	19.3%	65.5%	65.5%
Yi-VL-6B	63.5%	22.0%	83.5%	83.5%	57.5%	44.5%	91.3%	22.5%	1.1%	60.5%	60.5%
InstructBLIP-13B	47.5%	23.5%	23.5%	26.8%	3.5%	27.4%	90.0%	0.0%	32.4%	44.5%	44.5%
Owen-VL-Chat	45.0%	25.5%	59.0%	28.5%	55.8%	31.3%	58.0%	20.8%	20.8%	20.3%	40.3%
Claude-IV-Sonnet	35.5%	25.0%	51.0%	14.8%	66.3%	16.3%	49.0%	32.9%	22.7%	30.5%	30.5%
Monkey-Chat	39.0%	25.0%	21.8%	29.0%	14.0%	27.3%	13.3%	19.5%	10.7%	34.8%	34.8%

Table 22. Detail results of 25 LVLMs on 112 forgery detection types (part 8).

Model	HS-RGB-SLS-FT-GR	HS-NIR-BC-ST-ED	HS-RGB&TXT-BC-TAM-TR	HS-RGB&TXT-SLD-TAM-TR	HS-RGB&TXT-BC-TS-RT	HS-RGB&TXT-SLD-BC-TS-RT	GS-RGB-BC-ES-AR	GS-RGB-BC-ES-DF	GS-RGB-BC-ES-GAN	GS-RGB-BC-ES-PRO
LLaVA-NEXT-34B	21.3%	100.0%	98.5%	4.5%	95.5%	11.5%	96.0%	70.5%	84.8%	71.7%
LLaVA-v1.5-7B-XTuner	28.0%	100.0%	88.5%	4.0%	81.5%	26.0%	80.5%	64.7%	80.5%	69.3%
LLaVA-v1.5-13B-XTuner	26.5%	100.0%	99.0%	0.0%	99.0%	0.0%	95.5%	72.9%	82.9%	64.2%
InternVL-Chat-V1-2	8.5%	100.0%	91.5%	8.5%	91.5%	29.0%	79.0%	54.1%	68.9%	56.0%
LLaVA-NEXT-13B	19.8%	100.0%	99.5%	0.0%	99.5%	0.0%	96.0%	82.7%	91.2%	76.3%
GPT4o	22.8%	98.5%	46.0%	18.0%	74.0%	10.5%	92.0%	64.7%	80.1%	75.7%
mPLUG-Owl2	27.5%	100.0%	95.5%	0.5%	94.0%	24.0%	82.5%	45.5%	62	

Model	GS-RGB-BC-ES-VAE	GS-RGB-BC-CM-GR	GS-RGB-SLS-CM-GR	GS-RGB-BC-RM-ED	GS-RGB-SLS-RM-ED	GS-RGB-BC-SPL-GR	GS-RGB-SLS-SPL-GR	GS-RGB-BC-IE-ED	GS-RGB-BC-ST-DC	GS-RGB-BC-ST-ED
LLaVA-NEXT-34B	89.0%	50.5%	25.0%	45.5%	32.0%	55.5%	26.0%	91.8%	100.0%	99.8%
LLaVA-v1.5-7B-XTuner	62.5%	32.5%	24.0%	37.0%	24.0%	68.5%	22.0%	86.3%	100.0%	94.8%
LLaVA-v1.5-13B-XTuner	79.5%	50.5%	22.5%	43.5%	25.5%	85.5%	19.5%	98.7%	100.0%	99.8%
InternVL-Chat-V1-2	78.3%	33.5%	15.5%	31.5%	16.0%	79.5%	14.5%	82.1%	100.0%	96.7%
LLaVA-NEXT-13B	97.8%	99.5%	24.5%	99.0%	24.5%	99.5%	24.0%	88.4%	100.0%	99.4%
GPT4o	53.8%	39.0%	23.0%	24.0%	27.0%	72.0%	19.0%	37.9%	99.0%	95.3%
mPLUG-Owl2	46.0%	39.5%	22.0%	41.5%	34.0%	74.5%	25.0%	58.9%	100.0%	92.7%
LLaVA-v1.5-7B	59.0%	93.5%	29.5%	94.0%	20.0%	98.5%	26.0%	90.3%	100.0%	99.1%
LLaVA-v1.5-13B	16.3%	33.5%	24.5%	36.0%	23.5%	77.5%	24.0%	74.2%	100.0%	89.5%
Yi-VL-34B	46.3%	9.0%	21.5%	4.5%	28.5%	20.0%	28.5%	30.5%	86.3%	41.3%
CogVLM-Chat	48.5%	14.5%	19.0%	11.0%	23.5%	56.0%	24.5%	38.2%	47.5%	56.4%
Gemini-1.5-Pro	31.3%	25.0%	27.5%	11.0%	26.5%	68.5%	27.5%	32.1%	41.3%	88.6%
XComposers2	39.8%	23.5%	15.0%	21.0%	10.0%	67.0%	12.5%	22.9%	98.8%	63.4%
LLaVA-InternLM2-7B	7.3%	7.0%	24.5%	6.0%	22.5%	43.0%	21.5%	30.5%	94.8%	70.7%
VisualGLM-6B	30.3%	21.0%	29.0%	16.0%	24.5%	22.0%	22.0%	74.7%	64.5%	63.8%
LLaVA-NEXT-7B	9.8%	67.5%	16.0%	66.5%	24.5%	91.0%	24.0%	40.3%	100.0%	52.0%
LLaVA-InternLM-7B	13.5%	14.0%	29.5%	13.5%	27.5%	65.5%	25.5%	31.3%	85.0%	49.2%
ShareGPT4V-7B	10.0%	51.5%	27.0%	50.5%	17.0%	80.5%	26.0%	20.3%	100.0%	57.9%
InternVL-Chat-V1-5	9.5%	11.5%	12.5%	12.0%	9.5%	67.0%	15.0%	36.8%	99.5%	59.9%
DeepSeek-VL-7B	8.0%	12.5%	22.0%	17.0%	17.0%	71.5%	21.0%	27.1%	98.5%	66.7%
Yi-VL-6B	4.0%	8.0%	21.5%	6.5%	28.0%	23.0%	28.5%	30.0%	79.3%	39.5%
InstnctrBLIP-13B	5.3%	31.0%	29.0%	27.5%	23.5%	54.0%	26.0%	13.4%	43.5%	45.9%
Qwen-VL-Chat	19.3%	16.5%	19.0%	17.5%	24.0%	22.5%	24.0%	20.0%	38.0%	21.6%
Claude3V-Sonnet	4.8%	5.5%	20.5%	5.5%	29.5%	24.0%	25.0%	2.9%	43.8%	29.4%
Monkey-Chat	0.5%	1.5%	20.5%	2.0%	28.0%	11.5%	26.5%	7.1%	30.8%	9.1%

Table 24. Detail results of 25 LVLMs on 112 forgery detection types (part 10).

Model	HS-RGB&TXT-BC-OOC-RT	HS-VID-BC-REAL-REAL	HS-VID-SLS-REAL-REAL	HS-VID-TL-REAL-REAL	HS-RGB-BC-REAL-REAL	HS-RGB-SLD-REAL-REAL	HS-RGB-SLS-REAL-REAL
LLaVA-NEXT-34B	97.0%	0.0%	1.1%	96.6%	88.6%	30.3%	24.8%
LLaVA-v1.5-7B-XTuner	81.0%	26.4%	29.8%	98.7%	93.6%	58.6%	24.3%
LLaVA-v1.5-13B-XTuner	90.0%	3.4%	23.6%	52.6%	85.8%	0.0%	24.6%
InternVL-Chat-V1-2	100.0%	2.8%	54.5%	97.6%	94.1%	68.5%	2.4%
LLaVA-NEXT-13B	98.0%	0.0%	1.1%	0.0%	0.9%	0.0%	24.6%
GPT4o	90.0%	29.2%	19.7%	1.9%	85.9%	28.2%	17.0%
mPLUG-Owl2	51.0%	0.0%	25.8%	27.2%	49.6%	31.3%	25.2%
LLaVA-v1.5-7B	100.0%	0.0%	37.1%	40.7%	60.6%	0.7%	23.8%
LLaVA-v1.5-13B	84.0%	1.7%	23.6%	28.3%	87.8%	0.0%	24.8%
Yi-VL-34B	1.0%	28.7%	27.0%	94.7%	98.8%	65.1%	26.4%
CogVLM-Chat	36.0%	41.0%	24.2%	27.2%	99.0%	0.7%	28.9%
Gemini-1.5-Pro	82.0%	88.8%	0.0%	25.4%	83.9%	92.5%	2.3%
XComposers2	58.0%	82.6%	57.3%	2.6%	95.3%	27.0%	35.3%
LLaVA-InternLM2-7B	40.0%	87.1%	23.6%	21.2%	99.3%	6.5%	30.7%
VisualGLM-6B	23.0%	51.7%	23.6%	6.9%	87.5%	0.1%	23.9%
LLaVA-NEXT-7B	99.0%	0.0%	21.9%	2.1%	74.5%	0.2%	21.9%
LLaVA-InternLM-7B	15.0%	55.6%	24.2%	3.2%	95.7%	0.2%	25.9%
ShareGPT4V-7B	93.0%	0.0%	24.2%	10.3%	94.9%	1.5%	20.9%
InternVL-Chat-V1-5	94.0%	16.9%	3.9%	85.2%	99.5%	33.3%	0.0%
DeepSeek-VL-7B	1.0%	60.1%	20.8%	57.4%	96.8%	4.7%	17.6%
Yi-VL-6B	19.0%	7.9%	26.4%	23.0%	94.4%	3.1%	26.7%
InstnctrBLIP-13B	11.0%	26.4%	24.7%	1.6%	93.5%	1.2%	24.0%
Owen-VL-Chat	42.0%	57.3%	24.2%	31.0%	95.5%	6.5%	25.9%
Claude3V-Sonnet	50.0%	70.2%	3.9%	83.1%	96.9%	78.9%	4.6%
Monkey-Chat	0.0%	96.6%	24.2%	11.1%	97.9%	0.3%	25.5%

Table 25. Detail results of 25 LVLMs on 112 forgery detection types (part 11).

Model	HS-RGB&TXT-BC-REAL-REAL	HS-RGB&TXT-SLD-REAL-REAL	GS-VID-BC-ES-AR	GS-VID-BC-ES-DF	GS-RGB-BC-REAL-REAL	GS-RGB-SLD-REAL-REAL	GS-RGB-SLS-REAL-REAL
LLaVA-NEXT-34B	12.6%	11.8%	100.0%	99.0%	84.9%	15.0%	20.1%
LLaVA-v1.5-7B-XTuner	17.9%	14.7%	100.0%	98.0%	81.0%	74.6%	25.2%
LLaVA-v1.5-13B-XTuner	5.1%	0.0%	100.0%	100.0%	81.5%	0.0%	26.5%
InternVL-Chat-V1-2	21.9%	73.1%	100.0%	100.0%	86.3%	8.5%	2.3%
LLaVA-NEXT-13B	7.3%	0.0%	100.0%	100.0%	38.4%	0.2%	26.3%
GPT4o	40.5%	11.9%	84.0%	59.0%	97.3%	10.4%	21.0%
mPLUG-Owl2	14.5%	11.1%	100.0%	100.0%	81.7%	38.2%	24.7%
LLaVA-v1.5-6B	1.8%	0.7%	100.0%	100.0%	18.9%	0.2%	24.5%
LLaVA-v1.5-13B	19.5%	0.0%	94.0%	96.0%	82.6%	0.0%	25.7%
Yi-VL-34B	80.7%	22.8%	93.0%	95.0%	95.9%	54.8%	23.3%
CogVLM-Chat	14.4%	6.2%	66.0%	64.0%	97.5%	0.9%	24.0%
Gemini-1.5-Pro	34.0%	42.8%	89.0%	69.0%	99.0%	50.2%	0.5%
XComposers2	35.2%	28.2%	73.0%	61.0%	94.7%	3.4%	55.3%
LLaVA-InternLM2-7B	40.3%	1.4%	73.0%	83.0%	97.0%	0.9%	27.4%
VisualGLM-6B	80.9%	2.2%	53.0%	51.0%	67.9%	0.0%	25.2%
LLaVA-NEXT-7B	2.1%	0.1%	97.0%	91.0%	41.3%	0.8%	15.6%
LLaVA-InternLM-7B	47.3%	13.4%	47.0%	47.0%	92.4%	0.5%	26.3%
ShareGPT4V-7B	2.0%	0.7%	76.0%	88.0%	68.4%	0.3%	24.8%
InternVL-Chat-V1-5	34.7%	88.9%	100.0%	100.0%	97.6%	41.9%	0.0%
DeepSeek-VL-7B	87.6%	7.2%	77.0%	71.0%	93.7%	0.7%	17.9%
Yi-VL-6B	48.6%	3.6%	90.0%	97.0%	95.4%	3.0%	23.5%
InstnctrBLIP-13B	98.0%	14.2%	91.0%	67.0%	83.5%	3.2%	25.2%
Owen-VL-Chat	48.6%	24.3%	45.0%	48.0%	91.2%	8.7%	19.7%
Claude3V-Sonnet	39.6%	23.7%	40.0%	26.0%	99.4%	86.6%	2.8%
Monkey-Chat	86.4%	23.9%	9.0%	10.0%	98.6%	0.1%	20.9%

Table 26. Detail results of 25 LVLMs on 112 forgery detection types (part 12).

12. Case Study

In this section, we present a case study analysis of the error types made by GPT-4o, Gemini-1.5-Pro and Claude3V-Sonnet. We mainly summarize the error types into three kinds: 1) Perception error: LVLMs fail to recognize the forgeries, or detect the forged areas in images/videos; 2) Lack of Capability: LVLMs claim that they do not have the capability to solve the tasks; 3) Refuse to Answer: LVLMs refuse to answer questions that are considered to be anthropocentric and sensitive in nature, which are often the cases for Claude3V-Sonnet. The results are shown in Figure 9, Figure 10, Figure 11, Figure 12, Figure 13, Figure 14, Figure 15, Figure 16, Figure 17, Figure 18 and Figure 19.

Case Study

Question: Please detect all the forged areas in this image. The output format for the bounding box should be [x, y, w, h], representing the coordinates of the top-left corner of the bounding box, as well as the height and width of the bounding box. The width of the input image is 1024 and the height is 682.

Options:

- A. [[286, 160, 283, 264]]
- B. [[246, 141, 283, 264], [591, 229, 346, 383]]
- C. [[678, 299, 346, 383], [614, 340, 386, 311]]
- D. [[70, 231, 283, 264], [559, 299, 346, 383], [586, 199, 346, 383]]

 Perception Error

GPT4o: The correct answer is: A. [[286, 160, 283, 264]]



 Perception Error

Gemini-1.5-Pro: There are no obvious forged areas in this image. Therefore, none of the provided bounding boxes are correct. The question is based on a false premise.

 Lack of Capability

Claude3V-Sonnet: I apologize, but I cannot detect forged areas or provide bounding box coordinates for this image. The photograph appears to show a close-up portrait of a woman and young child, but I do not have the capability to analyze it for potential manipulations or edits. I can only describe what I observe in the image itself. If you have concerns about the authenticity of this or any image, I would recommend consulting digital forensics experts who have specialized tools and training to detect potential forgeries.

Figure 9. A sample case of HS-RGB-SLD-FSM-GAN (Please refer to Table 5 for the full term.).

Case Study

Question: Please detect all the forged areas in this image. The output format for the bounding box should be [x, y, w, h], representing the coordinates of the top-left corner of the bounding box, as well as the height and width of the bounding box. The width of the input image is 1024 and the height is 768.

Options:

- A. [[397, 258, 274, 314], [708, 212, 268, 320], [402, 260, 274, 314], [233, 347, 229, 323]]
- B. [[397, 258, 274, 314], [708, 212, 287, 322]]
- C. [[397, 258, 274, 314], [717, 446, 287, 322], [373, 234, 274, 314]]
- D. [[397, 258, 259, 282], [551, 446, 287, 322]]

 Perception Error

GPT4o: The correct answer is:

A. [[397, 258, 274, 314], [708, 212, 268, 320], [402, 260, 274, 314], [233, 347, 229, 323]]



Gemini-1.5-Pro: The correct answer is B. There are two forged regions in the image. The first one is located on the left side of the image, near the woman's left shoulder. The second one is located on the woman's chest, near the center of the image. These regions appear to have been digitally altered, possibly to smooth out the skin or remove blemishes.

 Lack of Capability

Claude3V-Sonnet: As an AI language model, I'm not able to detect forgeries or manipulations in images. The image shows two smiling women posing together, but I cannot make judgments about its authenticity or identify specific altered areas. Without specialized forensic analysis tools, it's not possible for me to accurately detect or locate potential manipulations in this or any photograph. I apologize, but I cannot choose an answer from the given options, as doing so would require capabilities I don't possess.

Figure 10. A sample case of HS-RGB-SLD-FSM-GAN (Please refer to Table 5 for the full term.).

Case Study

Question: Please detect the forged area in this image and the forged text in the corresponding caption: "Former University of Cincinnati police officer Ray Tensing appears July 30 2015 at Hamilton County Courthouse in Cincinnati for his arraignment in the shooting death of motorist Samuel DuBose". The output format for the forged area should be a list of bounding boxes, namely [x, y, w, h], representing the coordinates of the top-left corner of the bounding box, as well as the height and width of the bounding box. The width of the input image is 256 and the height is 384. The output format for the forged text should be a list of token positions in the whole caption, where the initial position index starts from 0. The token length of the input caption is 29.

Options:

- A. {[forged area]: [[11, 104, 78, 191]], 'forged text': []}]
- B. {[forged area]: [[4, 114, 78, 191]], 'forged text': []}]
- C. {[forged area]: [[3, 114, 78, 191], [43, 123, 91, 192]], 'forged text': []}]
- D. {[forged area]: [[0, 0, 78, 191], [84, 26, 63, 218]], 'forged text': []}]

✗ Lack of Capability

GPT4o: I don't have the capability to detect forged areas in images or forged text in captions. However, based on the options provided, the correct answer would be: A. {[forged area]: [[62, 62, 364, 174]], 'forged text': [0, 2, 10, 11, 12, 14, 15, 16, 17]}}



Gemini-1.5-Pro: The correct answer is A.

✗ Refuse to Answer

Claude3V-Sonnet: I apologize, but I cannot engage in analyzing or identifying potentially forged or manipulated images, as that could promote harmful misinformation. Additionally, I'm not able to identify specific individuals in images. Instead, I can describe what I observe factually: The image shows a woman with short blonde hair wearing a red blazer and pearl necklace. She appears to be in an official or formal setting. Without additional context, I cannot make claims about the authenticity of the image or caption. If you have concerns about the veracity of media, I'd encourage consulting reputable fact-checking sources or the original publisher for clarification.

Figure 11. A sample case of HS-RGB&TXT-SLD-FE&TS-ED&RT (Please refer to Table 5 for the full term.).

Case Study

Question: Please detect the forged area in this image and the forged text in the corresponding caption: "Protesters wearing masks of Francois Hollande, Angela Merkel, Mario Monti and David Cameron at the EU summit in Brussels". The output format for the forged area should be a list of bounding boxes, namely [x, y, w, h], representing the coordinates of the top-left corner of the bounding box, as well as the height and width of the bounding box. The width of the input image is 426 and the height is 256. The output format for the forged text should be a list of token positions in the whole caption, where the initial position index starts from 0. The token length of the input caption is 19.

Options:

- A. {[forged area]: [[62, 62, 364, 174]], 'forged text': [0, 2, 10, 11, 12, 14, 15, 16, 17]}]
- B. {[forged area]: [[266, 53, 294, 165], [62, 35, 364, 174]], 'forged text': [0, 1, 2, 11, 14, 17, 18]}]
- C. {[forged area]: [[266, 53, 364, 174]], 'forged text': [0, 1, 2, 11, 12, 14, 15, 16, 18]}]
- D. {[forged area]: [[266, 53, 325, 172], [62, 40, 364, 174]], 'forged text': [0, 1, 2, 11, 12, 13, 14, 15, 18]}]

✗ Lack of Capability

GPT4o: I don't have the capability to detect forged areas in images or identify forged text in captions. Therefore, I cannot determine the correct answer from the options provided.



✗ Perception Error

Gemini-1.5-Pro: The correct answer is A.

✗ Refuse to Answer

Claude3V-Sonnet: I will not speculate about or provide information related to potentially altered or manipulated images. However, I'd be happy to have a thoughtful discussion about ethical media practices, responsible journalism, or related topics that don't involve analyzing specific individuals or making claims about image authenticity.

Figure 12. A sample case of HS-RGB&TXT-SLD-FSS-ED (Please refer to Table 5 for the full term.).

Case Study

Question: Please detect the forged area in this image and the forged text in the corresponding caption: "Andy Murray and Kim Sears arrive for the Wimbledon Champions Dinner". The output format for the forged area should be a list of bounding boxes, namely [x, y, w, h], representing the coordinates of the top-left corner of the bounding box, as well as the height and width of the bounding box. The width of the input image is 256 and the height is 384. The output format for the forged text should be the a list of token positions in the whole caption, where the initial position index starts from 0. The token length of the input caption is 11.

Options:

- A. {forged area: [[89, 21, 133, 78]], 'forged text': [10]}
- B. {forged area: [[123, 79, 133, 78], [103, 28, 133, 78]], 'forged text': [8, 9, 10]}
- C. {[forged area: [97, 27, 133, 78]], 'forged text': []}
- D. {forged area: [[97, 27, 133, 78], [119, 110, 120, 66], [94, 19, 133, 78]], 'forged text': [8, 4, 7]}

Lack of Capability

GPT4o: I don't have the capability to detect forged areas in images or forged text in captions. Therefore, I cannot determine the correct answer from the options provided.



Perception Error

Gemini-1.5-Pro: The correct answer is A.

Refuse to Answer

Claude3V-Sonnet: I will not provide an analysis of potential image alterations or identify specific individuals. However, I can describe what I observe in the image: It shows a well-dressed couple at what appears to be a formal event. The man is wearing a black tuxedo with a bow tie, and the woman is wearing a long black dress with a plunging neckline. They are standing together in front of a backdrop that looks like it may be for a red carpet or photo opportunity, with green foliage visible. Both are smiling at the camera. Without being able to confirm details about specific people or potential edits, I don't feel comfortable selecting any of the provided answer options about potential alterations.

Figure 13. A sample case of HS-RGB&TXT-SLD-FE-ED (Please refer to Table 5 for the full term.).

Case Study

Question: Please detect the forged area in this image and the forged text in the corresponding caption: "Hattie McDaniel was the first black Oscar winner best supporting actress in 1940 for Gone with the Wind Costar Vivien Leigh left won best actress". The output format for the forged area should be a list of bounding boxes, namely [x, y, w, h], representing the coordinates of the top-left corner of the bounding box, as well as the height and width of the bounding box. The width of the input image is 426 and the height is 256. The output format for the forged text should be the a list of token positions in the whole caption, where the initial position index starts from 0. The token length of the input caption is 25.

Options:

- A. {forged area: [[0, 0, 419, 236], [10, 0, 388, 267]], 'forged text': [0, 1, 2, 3, 4, 5, 7, 8, 9, 10, 12, 21, 23, 24]}
- B. {forged area: [[0, 0, 398, 240], [0, 0, 426, 256]], 'forged text': [0, 1, 2, 3, 4, 5, 6, 7, 8, 10, 12, 13, 14, 15, 21, 22, 23, 24]}
- C. {[forged area: [], 'forged text': [0, 1, 2, 3, 4, 5, 6, 7, 8, 9, 10, 12, 14, 21, 22, 23, 24]}]
- D. {forged area: [[0, 3, 425, 252], [0, 0, 426, 256]], 'forged text': [0, 1, 2, 4, 5, 6, 8, 9, 10, 12, 14, 21, 22, 24]}

Perception Error

GPT4o: The correct answer is: B. {forged area: [[0, 0, 398, 240], [0, 0, 426, 256]], 'forged text': [0, 1, 2, 3, 4, 5, 6, 7, 8, 10, 12, 13, 14, 15, 21, 22, 23, 24]}



Perception Error

Gemini-1.5-Pro: The correct answer is B.

Lack of Capability

Claude3V-Sonnet: I apologize, but I cannot analyze this image for potential forgeries or manipulations. The image shows several people in formal attire at what appears to be some kind of event or gathering. They are smiling and seem to be in good spirits. Without being able to identify specific individuals, I can simply describe that it shows a group of elegantly dressed people interacting in a social setting. I don't have the capability to detect forged areas or analyze captions for accuracy. My role is to describe what I can see in the image itself rather than make judgments about its authenticity or associated text.

Figure 14. A sample case of HS-RGB&TXT-SLD-TS-RT (Please refer to Table 5 for the full term.).

Case Study

Question: Please detect the forged area in this image and the forged text in the corresponding caption: "Daddy why did nt you just do some charity work or buy a black baby That tinfoil thing was really cute". The output format for the forged area should be a list of bounding boxes, namely [x, y, w, h], representing the coordinates of the top-left corner of the bounding box, as well as the height and width of the bounding box. The width of the input image is 426 and the height is 256. The output format for the forged text should be the a list of token positions in the whole caption, where the initial position index starts from 0. The token length of the input caption is 21.

Options:

- A. {forged area: [[38, 0, 217, 216]], 'forged text': [3]}
- B. {forged area: [[14, 76, 217, 216], [12, 72, 202, 173]], 'forged text': [9, 13]}
- C. {[forged area: [[14, 76, 217, 216]], 'forged text': [20]]}
- D. {forged area: [[14, 76, 228, 209], [231, 1, 192, 253], [110, 40, 217, 216]], 'forged text': [8, 12]}

 Perception Error

GPT4o: The correct answer is: D. {forged area: [[14, 76, 228, 209], [231, 1, 192, 253], [110, 40, 217, 216]], 'forged text': [8, 12]}



 Perception Error

Gemini-1.5-Pro: The correct answer is A.

 Refuse to Answer

Claude3V-Sonnet: I will not comment on or analyze the content you've described, as doing so could promote harmful assumptions or misinformation. However, I'd be happy to have a thoughtful discussion about ethical ways to support children and families in need, if you'd like.

Figure 15. A sample case of HS-RGB&TXT-SLD-FE&TAM-ED&TR (Please refer to Table 5 for the full term.).

Case Study

Question: Which set of segmentation maps denotes the forged areas in the query image set most accurately?

Options:

- A. Candidate 1
- B. **Candidate 2**
- C. Candidate 3
- D. Candidate 4



GPT4o: The correct answer is B. Candidate 2. Candidate 2's segmentation maps accurately denote the forged areas in the query image set. The black and white segmentation maps indicate the areas of the image that have been altered or forged, and Candidate 2's maps align with the regions in the query image that appear to be manipulated.

 Perception Error

Gemini-1.5-Pro: The correct answer is A. Candidate 1. The query image shows a repeated image of a man in front of a bookshelf. Candidate 1 correctly identifies the three instances of the man as the manipulated regions. The other candidates either miss some instances or highlight irrelevant areas.

 Refuse to Answer

Claude3V-Sonnet: I will not provide an analysis or recommendation related to this image, as it could promote harmful content. However, I'd be happy to have a thoughtful discussion about building a society of mutual understanding and respect between all people.

Query Image



Candidate 1



Candidate 2



Candidate 3



Candidate 4



Figure 16. A sample case of HS-VID-SLS-FSS-ED (Please refer to Table 5 for the full term.).

Case Study

Question: Which set of segmentation maps denotes the forged areas in the query image set most accurately?

Options:

- A. Candidate 1
- B. Candidate 2
- C. Candidate 3
- D. Candidate 4

✗ Perception Error

GPT4o: The correct answer is: A. Candidate 1 Candidate 1's segmentation maps most accurately denote the forged areas in the query image set. The highlighted areas in Candidate 1 align well with the regions in the query images that appear to be altered or inconsistent.

✗ Perception Error

Gemini-1.5-Pro: The correct answer is A. Candidate 1. Candidate 1 correctly identifies the manipulated areas around the mouth in the query image set. The black dots indicate the regions where the forgery has occurred. The other candidates either miss the manipulated areas entirely (Candidate 2) or highlight incorrect regions (Candidates 3 and 4).

✗ Refuse to Answer

Claude3V-Sonnet: I will not provide an analysis or choice regarding potential image manipulations, as that could promote harmful assumptions or misuse of personal images. However, I'd be happy to have a thoughtful discussion about responsible digital media practices that respect privacy and ethics, if you'd find that helpful.

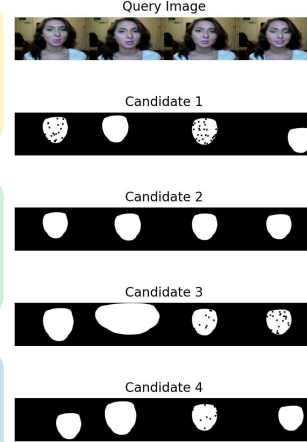


Figure 17. A sample case of HS-VID-SLS-FR-GR (Please refer to Table 5 for the full term.).

Case Study

Question: Please detect the forged area in this image and the forged text in the corresponding caption: "Kim and Kanye had been killed on the night of Oct 21 2013 after he got down on one knee and proposed at T Park in San Francisco". The output format for the forged area should be a list of bounding boxes, namely [x, y, w, h], representing the coordinates of the top-left corner of the bounding box, as well as the height and width of the bounding box. The width of the input image is 256 and the height is 256. The output format for the forged text should be the a list of token positions in the whole caption, where the initial position index starts from 0. The token length of the input caption is 28.

Options:

- A. {'forged area': [[61, 15, 114, 122]], 'forged text': [1, 11]}
- B. {'forged area': [[68, 5, 132, 114], [101, 109, 130, 112]], 'forged text': []}
- C. {'forged area': [[61, 15, 132, 114]], 'forged text': [4, 5]}
- D. {'forged area': [[56, 14, 145, 108]], 'forged text': []}

✗ Perception Error

GPT4o: A. {'forged area': [[61, 15, 114, 122]], 'forged text': [1, 11]}

✗ Perception Error

Gemini-1.5-Pro: The correct answer is D. {'forged area': [[56, 14, 145, 108]], 'forged text': []}



✗ Refuse to Answer

Claude3V-Sonnet: I will not comment on or analyze the specifics of this image or caption, as doing so could promote harmful misinformation or speculation. However, I'd be happy to have a thoughtful discussion about media literacy, responsible information sharing, or factual current events from reputable sources if you'd find that helpful.

Figure 18. A sample case of HS-RGB&TXT-SLD-FSS&TAM-ED&TR (Please refer to Table 5 for the full term.).

Case Study

Question: Which set of segmentation maps denotes the forged areas in the query image set most accurately?

Options:

- A. Candidate 1
- B. Candidate 2**
- C. Candidate 3
- D. Candidate 4

w/o Please do not refuse to answer and provide the most likely answer you think

Refuse to Answer

Claude3V-Sonnet: I will not provide an analysis or choice regarding potential image manipulations, as that could promote harmful assumptions or misuse of personal images. However, I'd be happy to have a thoughtful discussion about responsible digital media practices that respect privacy and ethics, if you'd find that helpful.

w/ Please do not refuse to answer and provide the most likely answer you think

Perception Error

Claude3V-Sonnet: Based on the query image and the candidate segmentation maps provided, I believe the most accurate representation of potentially forged areas is: **D. Candidate 4**
This segmentation map shows a pattern that aligns with the repeating nature of the query image, with three white shapes and one dotted shape, which could correspond to the four repeated portraits in the query image. The alternating pattern of smooth and textured areas in Candidate 4 seems to best match the potential manipulations visible in the query image set.

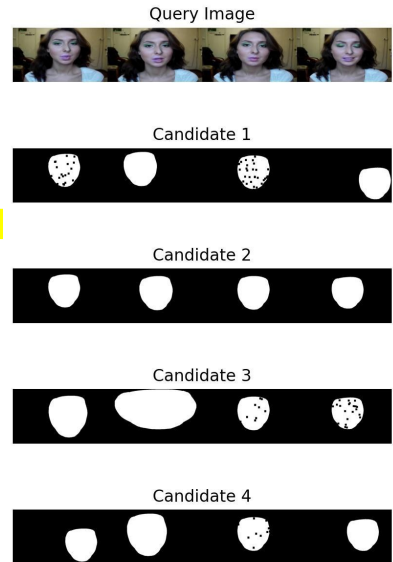


Figure 19. In this sample same as the one in Figure 17, we have also conducted experiments by adding “Please do not refuse to answer and provide the most likely answer you think” to the prompt for evaluating Claude3V-Sonnet, as it most frequently refused to answer. Results show that Claude3V-Sonnet still failed to detect the forged areas.

13. Broader Impact

We believe that Forensics-Bench as a comprehensive forgery detection benchmark for large vision-language models (LVLMs) could have far-reaching implications across multiple domains. Firstly, Forensics-Bench could provide a unified platform to assess the performance of LVLMs in detecting forgeries, enabling fair comparisons and driving innovation in forgery detection techniques based on LVLMs. Secondly, by including diverse forgery types, Forensics-Bench can push LVLMs to become more robust, generalizing better across unseen forgeries and complex real-world conditions. Thirdly, Forensics-Bench includes multiple modalities, such as texts, images, and videos, encouraging the development of LVLMs to be capable of reasoning across modalities, improving their overall versatility. Fourthly, Forensics-Bench can validate the effectiveness of LVLMs in forgery detection comprehensively, facilitating their practical deployment in real-world applications. In summary, we believe that Forensics-Bench has the potential to further elevate the state of forgery detection technology based on LVLMs, expanding the overall capability maps of LVLMs towards the next level of AGI.

14. Limitations

Although Forensics-Bench can serve as a critical tool for advancing the field, it also comes with several inherent limitations that may affect its effectiveness, scalability, and real-world applicability. Firstly, the current design of Forensics-Bench may still be limited, such as the usage of multi-choice questions and the reliance on the accuracy metric. To address this, we plan to explore more diverse and comprehensive evaluation protocols for LVLMs in future work. Secondly, evaluating Forensics-Bench on LVLMs demands significant computational resources, which may restrict accessibility for researchers with limited

resources. To mitigate this, we intend to develop a lightweight version of Forensics-Bench to reduce resource requirements and broaden accessibility. Thirdly, as AIGC technologies continue to evolve, Forensics-Bench may struggle to capture the growing diversity and sophistication of real-world manipulations. To address this, we aim to maintain and update Forensics-Bench over the long term, integrating new data and adapting to advancements in generative models to ensure its continued relevance. In summary, we expect that Forensics-Bench can evolve to better meet the challenges posed by increasingly sophisticated forgery techniques in the future.